The EMBO Journal (2006) 25, 232–243 | © 2006 European Molecular Biology Organization | All Rights Reserved 0261-4189/06
www.embojournal.org

THE EMBO JOURNAL

The two *Drosophila* cytochrome C proteins can function in both respiration and caspase activation

Eli Arama[1], Maya Bader[1], Mayank Srivastava[2], Andreas Bergmann[2] and Hermann Steller[1,*]

[1]Strang Laboratory of Cancer Research, Howard Hughes Medical Institute, The Rockefeller University, New York, NY, USA and [2]Department of Biochemistry and Molecular Biology, The University of Texas MD Anderson Cancer Center, Houston, TX, USA

Cytochrome C has two apparently separable cellular functions: respiration and caspase activation during apoptosis. While a role of the mitochondria and cytochrome C in the assembly of the apoptosome and caspase activation has been established for mammalian cells, the existence of a comparable function for cytochrome C in invertebrates remains controversial. *Drosophila* possesses two cytochrome *c* genes, *cyt-c-d* and *cyt-c-p*. We show that only *cyt-c-d* is required for caspase activation in an apoptosis-like process during spermatid differentiation, whereas *cyt-c-p* is required for respiration in the soma. However, both cytochrome C proteins can function interchangeably in respiration and caspase activation, and the difference in their genetic requirements can be attributed to differential expression in the soma and testes. Furthermore, orthologues of the apoptosome components, Ark (Apaf-1) and Dronc (caspase-9), are also required for the proper removal of bulk cytoplasm during spermatogenesis. Finally, several mutants that block caspase activation during spermatogenesis were isolated in a genetic screen, including mutants with defects in spermatid mitochondrial organization. These observations establish a role for the mitochondria in caspase activation during spermatogenesis.
The EMBO Journal (2006) **25,** 232–243. doi:10.1038/sj.emboj.7600920; Published online 15 December 2005
Subject Categories: development; differentiation & death
Keywords: apoptosis; caspase; cytochrome *c*; *Drosophila*; spermatogenesis

Introduction

Apoptosis is a morphologically distinct form of active cellular suicide that serves to eliminate unwanted and potentially dangerous cells (Thompson, 1995; Jacobson *et al*, 1997; Hengartner, 2000; Meier *et al*, 2000a; Baehrecke, 2002; Nelson and White, 2004). The key enzymes responsible for the execution of apoptosis are an evolutionarily conserved family of cysteine proteases known as caspases (Salvesen, 2002; Degterev *et al*, 2003; Abraham and Shaham, 2004). Caspases are present in an inactive or weakly active state in virtually all cells of higher metazoans, and their activity is carefully regulated by both activators and inhibitors (Song and Steller, 1999; Salvesen and Abrams, 2004). In vertebrates, the mitochondria play an important role in the control of apoptosis: they release cytochrome C and other pro-apoptotic proteins in response to various death signals (Zou *et al*, 1997; Green and Reed, 1998; Benedict *et al*, 2000; Larisch *et al*, 2000; Wang, 2001). In the cytosol, cytochrome C binds to Apaf-1 (Zou *et al*, 1997) which in turn promotes the assembly of a multiprotein complex, termed the 'apoptosome', and caspase-9 activation (Rodriguez and Lazebnik, 1999; Adams and Cory, 2002; Cain *et al*, 2002; Salvesen and Renatus, 2002). In the ensuing 'caspase cascade', many intracellular substrates are cleaved and apoptosis is executed (Slee *et al*, 1999; Riedl and Shi, 2004). However, the exact physiological role of cytochrome C for caspase activation remains to be determined, and a recent report on a mutant cytochrome *c* that fails to activate Apaf-1 in the mouse suggests that cytochrome C is required for caspase activation in only some mammalian cell types (Hao *et al*, 2005). In invertebrates, any role of cytochrome C for the activation of caspases has remained highly controversial (Kornbluth and White, 2005). Whereas RNAi experiments in *Drosophila* S2 cells have failed to reveal a role for cytochrome C in apoptosis, other reports suggest that cytochrome C may promote caspase activation (Dorstyn *et al*, 2002, 2004; Zimmermann *et al*, 2002). *Drosophila* contains two Apaf-1 isoforms: one with a WD40 repeat domain, the target for cytochrome C binding, and another lacking this domain, similar to *Caenorhabditis elegans* Ced-4. The large isoform can directly bind cytochrome C *in vitro* and promote cytochrome C-dependent caspase activation in lysates from developing embryos (Kanuka *et al*, 1999). Furthermore, an overt alteration in the cytochrome C immuno-staining can be detected in doomed cells in some *Drosophila* tissues, and the mitochondria from apoptotic cells can activate cytosolic caspases (Varkey *et al*, 1999). Finally, disruption of one of the two *Drosophila* cytochrome *c* genes, *cyt-c-d*, is associated with a failure to activate caspases in an apoptosis-like process during sperm terminal differentiation in *Drosophila* (Arama *et al*, 2003). In this process, also known as spermatid individualization, the majority of cytoplasm and cellular organelles are eliminated from the developing spermatids in an apoptosis-like process that requires caspase activity (Arama *et al*, 2003). However, it was suggested that the mutants used in our previous study may also affect other genes located in the vicinity of the *cyt-c-d* locus (Huh *et al*, 2004). Here, in order to rigorously address this issue, we conducted a series of genetic and transgenic rescue experiments that unequivocally establish a role of cytochrome C for caspase activation during *Drosophila* spermatogenesis. First, we isolated a point mutation in *cyt-c-d* that is defective in caspase activation. Next, we demonstrated that transgenic expression of *cyt-c-d* restores effector caspase activation and

*Corresponding author. Strang Laboratory of Cancer Research, Howard Hughes Medical Institute, The Rockefeller University, 1230 York Avenue, New York, NY 10021, USA. Tel.: +1 212 327 7075; Fax: +1 212 327 7076; E-mail: steller@rockefeller.edu

Received: 4 October 2005; accepted: 22 November 2005; published online: 15 December 2005

rescues all the sterility phenotypes associated with various *cyt-c-d* mutant alleles. We also investigated the possibility that *cyt-c-p* functions specifically in respiration, whereas *cyt-c-d* plays a role in caspase regulation. To our surprise, we found that expression of either *cyt-c-d* or *cyt-c-p* can restore caspase activation in *cyt-c-d*-deficient spermatids, demonstrating that both proteins are functionally equivalent. Other apoptosome proteins in *Drosophila*, Ark (Apaf-1) and Dronc (caspase-9) are also required for spermatid individualization, and their mutant phenotypes are similar to spermatids with a block in caspase activity. Surprisingly, however, we can still detect some active caspase-3 staining in these mutant testes, suggesting that cytochrome-C-d may function in yet other unknown pathways to promote caspase-3 activation. Finally, we have identified several mutants affecting spermatid mitochondria that provide a strong link between mitochondrial organization and caspase activation during sperm development.

Results

Mutations in cyt-c-d block caspase activation during spermatid individualization

In order to identify genes required for caspase activation during spermatid differentiation in *Drosophila*, we sought to identify mutants that lacked CM1 staining, which detects the active form of the effector casepase drICE (Baker and Yu, 2001). For this purpose, we screened an existing collection of more than 1000 male-sterile mutant lines defective in spermatid individualization that were previously identified among a collection of about 6000 viable mutants generated in the laboratory of Dr Charles Zuker (Koundakjian *et al*, 2004; Wakimoto *et al*, 2004). We stained dissected testes from each line with CM1 (see Supplementary data) and identified 33 lines that were CM1-negative. However, the vast majority of male-sterile lines remained CM1-positive, even though many displayed severe defects in spermatid individualization (e.g. Figure 1F). Therefore, consistent with our earlier observations (Arama *et al*, 2003), caspase activation at the onset of spermatid individualization appears to be independent of other aspects of sperm differentiation, such as the assembly of the individualization complex or its movement. One of the mutants, line *Z2-1091*, failed to complement the sterility of bln^1, a *P*-element insertion in *cyt-c-d,* and was CM1-negative as a homozygote, in *trans* to a small deletion removing the *cyt-c-d* locus (*Df*(2L)*Exel6039*), or in *trans* to the $cyt\text{-}c\text{-}d^{bln1}$ allele (Figure 1C–E). In contrast, *Z2-1091* complemented the lethality of *K13905*, a *P*-element insertion in *cyt-c-p*, and *K13905* complemented the sterility of *Z2-1091*. Genomic sequence analyses of the transcription units of both *cyt-c-d* and *cyt-c-p* in *Z2-1091* flies revealed a point mutation of TGG→TGA at codon 62 in *cyt-c-d*, causing a change of Trp62 into a stop codon that results in a truncation of almost half of the protein (Figure 1H). We will henceforth refer to this allele as $cyt\text{-}c\text{-}d^{Z2-1091}$. Given the molecular nature of $cyt\text{-}c\text{-}d^{Z2-1091}$, it is very unlikely that this allele affects the function of genes adjacent to *cyt-c-d* (see below).

Effector caspases, such as drICE, can display DEVD cleaving activity (Fraser *et al*, 1997). Therefore, we asked whether wild-type adult testes also contain DEVDase activity, and whether this activity is affected in *cyt-c-d* mutant testes. Lysates of wild-type testes indeed display detectable levels of DEVDase activity, which were significantly reduced upon treatment with the potent DEVDase inhibitor Z-VAD.fmk (Figure 1G). Importantly, this activity was highly reduced in $cyt\text{-}c\text{-}d^{Z2-1091}$ mutant testes (Figure 1G). These results provide independent evidence for effector caspase activity in wild-type sperm, and they support a role of cytochrome C-d in caspase activation in this system.

Because of the cytological proximity between *cyt-c-d* and *cyt-c-p* (241 bp maximum between the end of the 3′ UTR of *cyt-c-d* and the beginning of the 5′ UTR of *cyt-c-p*) there is a possibility that the bln^1 *P*-element insertion in *cyt-c-d* might also interfere with the expression of *cyt-c-p* (Huh *et al*, 2004). In order to determine whether *cyt-c-p* expression was altered in $cyt\text{-}c\text{-}d^{bln1}$, we performed RT–PCR analyses with RNA from wild-type (yw) and $cyt\text{-}c\text{-}d^{bln1}$ adult flies using two sets of primers for each gene specific for either the 5′ UTRs (upper panel of Figure 1I) or 3′ UTRs (lower panel of Figure 1I) of *cyt-c-d* and *cyt-c-p*. In agreement with our previous Northern results, no *cyt-c-d* RNA was detected in $cyt\text{-}c\text{-}d^{bln1}$ flies, confirming that bln^1 is a null allele of *cyt-c-d*. In contrast, *cyt-c-p* is expressed in both wild-type and $cyt\text{-}c\text{-}d^{bln1}$ flies.

Both cyt-c-d and cyt-c-p can rescue caspase activation, spermatid individualization, and the sterility of bln^1 and Z2–1091 adult males

Although the sequence of *cyt-c-d* and *cyt-c-p* proteins is highly conserved, they are not identical (Figure 1H). In addition, mutations in each gene display distinct phenotypes (Arama *et al*, 2003). This raises the possibility that both proteins may have distinct functions in respiration (cytochrome C-p) and caspase activation/apoptosis (cytochrome C-d). To test this hypothesis, we first asked whether expression of *cyt-c-p* in developing spermatids is able to substitute for the loss of *cyt-c-d*. In order to drive expression of transgenes in the male germ line, we constructed an expression vector composed of the *hsp83* promoter followed by the 5′ and 3′ UTRs of *cyt-c-d*, which are important for the proper temporal regulation of *cyt-c-d* translation in spermatids (Figure 2A, I; see Supplementary data; Arama and Steller, unpublished), and next we inserted the coding regions of either *cyt-c-d* (Figure 2A, II) or *cyt-c-p* (Figure 2A, III) between both UTRs and generated transgenic flies with these constructs. At least three independent transgenic lines for each of these constructs were crossed to $cyt\text{-}c\text{-}d^{bln1}$ or $cyt\text{-}c\text{-}d^{Z2-1091}$ flies, and the presence of the appropriate transgene was confirmed by genomic PCR (Figure 2F and data not shown). To validate expression of the transgenes, we performed RT–PCR analysis with testes RNA in a $cyt\text{-}c\text{-}d^{bln1}-/-$ background (Figure 2G and H). Finally, we examined the ability of these transgenes to rescue caspase activation, spermatid individualization, and male sterility in $cyt\text{-}c\text{-}d^{bln1}$ and $cyt\text{-}c\text{-}d^{Z2-1091}$ flies. As a control, transgenic flies containing 'empty vector' (including the *hsp83*-promotor with the 5′ and 3′ UTRs of *cyt-c-d* but without a coding region) were also generated (Figure 2A, I and G). As expected, no caspase activation was detected in testes of these control flies (Figure 2C, compare to the wild-type in Figure 2B). On the other hand, a transgene with the *cyt-c-d* open reading frame (ORF) fully rescued CM1-staining, spermatid individualization, and male fertility (Figure 2D, note the reappearance of cystic bulges (CBs) and waste bags (WBs), white and yellow arrows, respectively). This firmly establishes that both the caspase and sterility phenotypes

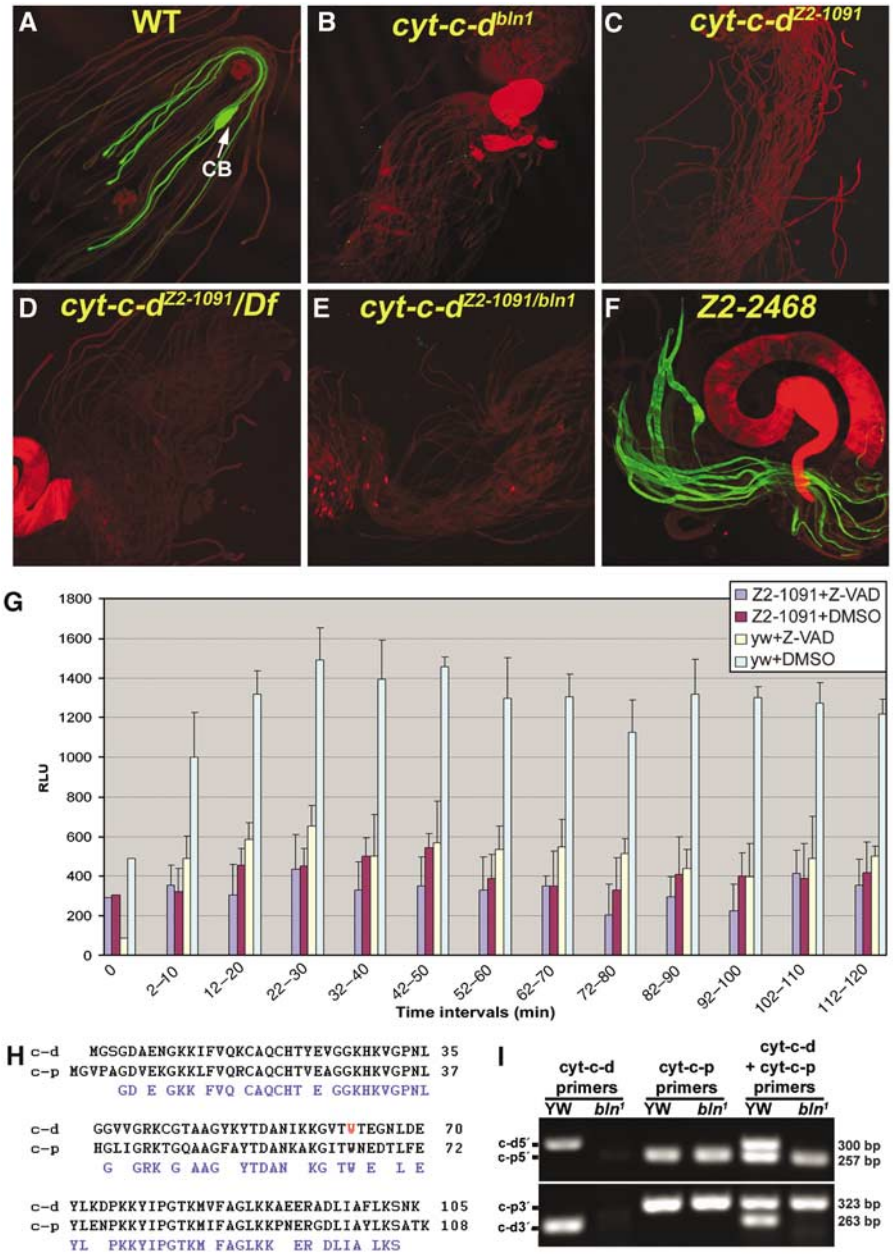

Figure 1 (**A–F**) Mutations in *cyt-c-d* block caspase activation and spermatid individualization. Visualization of active drICE with anti-cleaved caspase-3 antibody (CM1; green) in wild-type (A), *cyt-c-d*^{bln1} (B), *cyt-c-d*$^{Z2-1091}$ (C), *cyt-c-d*$^{Z2-1091}$/*DF*(2L)Exel6039 (D), *cyt-c-d*$^{Z2-1091}$/*cyt-c-d*^{bln1} (E), and *Z2-2468* (F). Whereas CM1-positive elongated spermatid cysts at different individualization stages can be readily seen in wild-type testes (A; white arrow pointing at a CB), no CM1-staining was detected in spermatids of flies homozygous for the *P*-element allele, *bln*^{1} (B) and the point mutation allele, *Z2-1091* (C). Similarly, spermatids of *Z2-1091* flies either *trans*-heterozygous to the small deficiency *Df*(2L)*Exel6039* (D) or to the *bln*^{1} allele (E) also displayed no CM1 staining. In contrast, the vast majority of male-sterile mutants with spermatid individualization defects display strong CM1 positive cysts (e.g. *Z2-2468*; F). To visualize all the spermatids, the testes were counter-stained with phalloidin that binds F-actin (red). (**G**) Caspase-3-like (DEVDase) activity is detected in wild-type testes, and is blocked either after treatment with the caspase-3 inhibitor Z-VAD.fmk or in *cyt-c-d*$^{Z2-1091}$−/− mutant testes. DEVDase activity, presented as relative luminescence units (RLU), was determined on Ac-DEVD-pNA substrate in 62 wild-type (*yw*) or *cyt-c-d*$^{Z2-1091}$−/− mutant testes treated with Z-VAD or left untreated (DMSO). Readings were obtained every 2 min, and each time interval represents an average (mean ± s.e.m.) of five readings (for more details also see the Supplementary data). Note that the levels of DEVDase activity in *cyt-c-d*$^{Z2-1091}$−/− mutant testes are highly similar to the corresponding levels in wild-type testes that were treated with Z-VAD. (**H**) Alignment of the predicted protein sequences of cytochrome C-d (c-d) and cytochrome C-p (c-p). Identical residues are indicated in the consensus (cons.) line. Cytochrome C-d and cytochrome C-p share 72% identity and 82% similarity. The tryptophan (W; red) at position 62 of cytochrome C-d is mutated to a stop codon in the *Z2-1091* allele. (**I**) RT–PCR analyses of *cyt-c-d* and *cyt-c-p* expression. After reverse transcription with adult flies RNA, PCR was performed using two sets of specific primers spanning the unique 5′ (upper panel) and 3′ (lower panel) UTRs of both *cyt-c-d* and *cyt-c-p*. Whereas *cyt-c-d* and *cyt-c-p* are expressed in wild-type flies (YW), only *cyt-c-p* is expressed in the *bln*^{1} flies, confirming that *bln*^{1} is a null allele of *cyt-c-d*.

seen in *cyt-c-d*^{bln1} and *cyt-c-d*$^{Z2-1091}$ mutant flies are strictly due to the loss of cytochrome *c* function, with no detectable contribution from adjacent genes.

We next tested the ability of *cyt-c-p* to functionally substitute for the loss of *cyt-c-d*. To our surprise, transgenic expression of *cyt-c-p* was equally effective in rescuing all

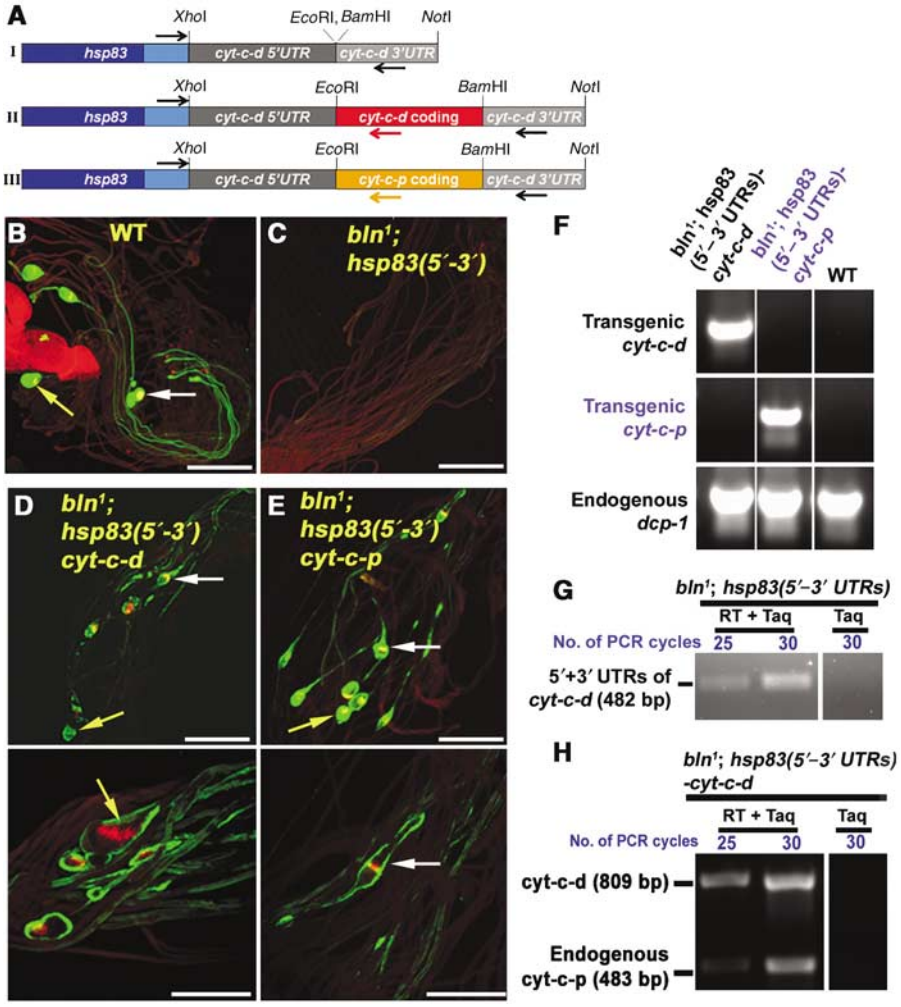

Figure 2 Both *cyt-c-d* and *cyt-c-p* can rescue the male sterile phenotypes of *cyt-c-d*$^{-/-}$ flies. (**A**) Schematic structure of the rescue constructs for *cyt-c-d*$^{-/-}$ male sterile flies. The promoter region (dark blue) and a portion of the 5′ UTR (light blue) of the *hsp83* gene were fused to the 5′ UTR followed by the 3′ UTR sequences of *cyt-c-d* and served as a control (I). The precise coding region sequences of either *cyt-c-d* (II) or *cyt-c-p* (III) were subcloned in between the 5′ and 3′ UTRs. (**B–E**) Ectopic expression of either *cyt-c-d* or *cyt-c-p* rescues caspase activation, spermatid individualization, and sterility of *cyt-c-d*^{bln1}−/− male flies. Similar to WT (B), CM1-positive spermatids (green), CBs (white arrows), and WBs (yellow arrows) are readily detected in transgenic lines of the *cyt-c-d*^{bln1}−/− background expressing either *cyt-c-d* (D) or *cyt-c-p* (E) coding regions. In contrast, no CM1-positive cysts are found in *cyt-c-d*^{bln1}−/− flies that ectopically express the control construct of *cyt-c-d* 5′–3′ UTRs alone (C). To visualize all the spermatids and the ICs, the testes were counter-stained with phalloidin that binds F-actin (spermatids are in weak red; ICs are in strong red or yellow and associated with CM1-positive spermatids; note that remnants of the testis sheath layer autofluoresce in strong red in B). Scale bars 200 μm (B–E, upper panels), and 100 μm (D, E, lower panels). (**F**) Integrations of the appropriate constructs into the genome were confirmed by genomic PCR analyses. The relative locations of the primers, which are indicated with forward black and reverse red (*cyt-c-d*; A, II) or reverse orange (*cyt-c-p*, A, III) arrows were used to amplify the fragments seen in the upper and middle panels in (F), respectively. For loading control, the *dcp-1* gene was amplified (lower panel in F). (**G, H**) Transcriptional expression from the transgenes was confirmed by RT–PCR analyses on RNA from testes of the indicated genotypes. The relative locations of the primers are indicated with black arrows in (A). Representative figures demonstrating exogenous expression of *cyt-c-d* 5′-3′ UTR sequences alone (G), and the exogenous expression of *cyt-c-d* coding region flanked by its UTR sequences (H). 'RT + Taq' and 'Taq' indicate reactions with reverse transcriptase or without it, respectively, to control for possible genomic DNA contamination. (H) Primers corresponding to the unique 5′ and 3′ UTRs of *cyt-c-p* and primers corresponding to the exogenous *cyt-c-d* sequences (see Materials and methods and black arrows in A) were used in the same reaction.

defects in *cyt-c-d*^{bln1} or and *cyt-c-d*$^{Z2-1091}$ males (Figure 2E). We conclude that both proteins have similar biochemical properties to promote caspase activation and spermatid individualization.

cyt-c-p is mainly somatic, whereas cyt-c-d is almost exclusively restricted to the male germ line

Our rescue results raise the question of why *cyt-c-d*$^{-/-}$ males are sterile if both cytochrome *c* genes are functionally equivalent. One possible explanation is distinct expression of the two genes, namely that *cyt-c-d* is testis-specific, whereas *cyt-c-p* may be restricted to the soma. To examine this possibility, we investigated the distribution of transcripts from both cytochrome *c* genes in the testis and the soma. For this purpose, comparative RT–PCR experiments were performed using specific primers in the unique 5′ and 3′ UTR sequences of *cyt-c-d* and *cyt-c-p* (Figure 3A). While *cyt-c-p* was highly expressed in the soma, *cyt-c-d* was only weakly expressed there (represented by adult females that lack testes). On the other hand, *cyt-c-d* expression was much

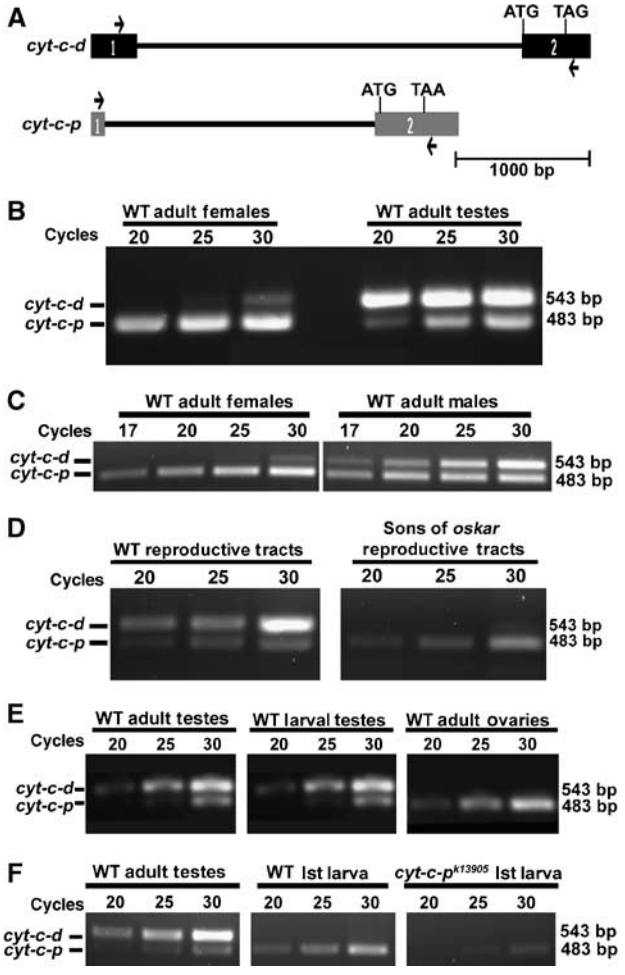

Figure 3 *cyt-c-d* is mainly expressed in the testis, while in contrast *cyt-c-p* is mainly expressed in the soma. (**A**) Schematic structure of the *Drosophila* cytochrome *c* genes. *cyt-c-d* and *cyt-c-p* display similar genomic organization of two exons (thick black and gray bars, respectively) separated by a relatively large intron (thin bar). In both of them, the coding region is restricted to the second exon (between the ATG and the stop codons). The locations of the primers used in the comparative RT–PCR experiments in (**B–E**) are indicated by arrows. (B) Analysis of *cyt-c-d* versus *cyt-c-p* expression in the testis and the soma. The above primers (arrows in A) to amplify either a 543-bp *cyt-c-d* fragment or a 483-bp *cyt-c-p* fragment were added to one reaction master-mix. The reaction was stopped at different cycle points to identify the linear amplification phase (20, 25, and 30 cycles are indicated). Note that the relative expression levels of *cyt-c-d* (strong) and *cyt-c-p* (weak) in the testis are switched in the soma, which is represented by adult female flies. (C) In the soma of both males and females, the expression levels of *cyt-c-d* are much lower than the levels of *cyt-c-p*. However, *cyt-c-d* levels are higher in adult males than in females. Note the PCR cycle number at which a band first becomes visible. (D) The expression of *cyt-c-d* is restricted to the male germ cells. While the expression of *cyt-c-p* is not affected in sons of *oskar* agametic testes, no *cyt-c-d* expression was detected. (E) *cyt-c-d* is expressed in premeiotic cells comprising the larval testis but not in ovaries. (**F**) *cyt-c-p* is exclusively expressed in first instar WT larva and is almost completely absent from the *cyt-c-p*^{k13905}−/−.

higher in testes than *cyt-c-p* (Figure 3B). We attribute the low levels of *cyt-c-p* in testes to the somatic cells present in this tissue (see below). Furthermore, although the expression of *cyt-c-d* in the soma of both males and females is much lower than the levels of *cyt-c-p*, *cyt-c-d* levels are much higher in adult males than in females, suggesting that the male germ cells provide the main contribution of *cyt-c-d* in the adult (Figure 3C). Our results suggest that the distinct phenotypes of *cyt-c-d* and *cyt-c-p* are mainly due to their restricted differential expression in the testis and the soma, respectively.

In addition to germ cells, the testis also contains somatic cells, such as the testicular wall, muscles cells, and cyst cells. To determine which testicular cell types express *cyt-c-d,* we first performed comparative RT–PCR analyses with RNA from reproductive tracts of *oskar* male mutants that are defective in germline development and lack germ cells in the adults. While both cytochrome *c* genes were expressed in wild type, only *cyt-c-p* was detected in the germ-cell-less reproductive tracts of sons of *oskar*$^{-/-}$ (Figure 3D). This indicates that *cyt-c-d* expression is restricted to the germ cells of the adult male. Next, we investigated the developmental stage at which *cyt-c-d* is expressed in the male germ line. For this purpose, we took advantage of the fact that testes of adult flies and third instar larvae differ in their repertoire of germ cells. While adult testes contain germ cells in a variety of developmental stages, the most developmentally advanced germ cells present in third instar larval testes are premeiotic spermatocytes. Interestingly, the patterns of *cyt-c-d* expression in both adult and larval testes are identical (Figure 3E), demonstrating that *cyt-c-d* mRNA accumulates before the entry of spermatocytes into meiosis.

The activation of apoptotic effector caspases, as visualized by CM1-staining, is not restricted to the male germ cells but can also be detected in nurse cells during oogenesis (Peterson *et al*, 2003). We considered the possibility that caspase activation in this system is also influenced by *cyt-c-d*. However, no abnormalities during oogenesis were detected in *cyt-c-d*$^{-/-}$ flies and the females are fertile (data not shown). Consistent with this idea, comparative RT–PCR analysis of adult ovaries revealed expression of *cyt-c-p* but not *cyt-c-d* (Figure 3E).

cyt-c-d expression is not detectable in early larva but can rescue the lethality of cyt-c-p$^{-/-}$ *mutant flies*

l(2)*k13905* flies contain a *P*-element insertion in the 5′ UTR of *cyt-c-p* and die as late embryos or early first instar larva (Arama *et al*, 2003). Using RT–PCR, we found that only *cyt-c-p* expression was detected in early first instar wild-type larvae, while a dramatic reduction was observed in the *cyt-c-p*^{k13905} mutants (Figure 3F). These results are consistent with the phenotypes of *cyt-c-d* (viable but male sterile) and *cyt-c-p* (early lethal) mutants.

Lethality of *cyt-c-p*^{k13905} homozygotes as well as *trans*-heterozygotes to *Df*(2L)*Exel6039*, a deletion in the region that includes both *cyt-c-p* and *cyt-c-d,* is consistent with the idea that *cyt-c-p* encodes the major cytochrome C responsible for respiration (Inoue *et al*, 1986). We investigated whether *cyt-c-d* could also function in respiration and rescue the early lethality of *cyt-c-p*$^{-/-}$ flies. Both cytochrome C proteins were ectopically expressed in *cyt-c-p*^{k13905} mutants using the GAL4-UAS system (Brand and Perrimon, 1993). The *Tub-Gal4* driver line was used to drive *cyt-c-p* and *cyt-c-d* expression throughout the lifespan of the fly. Notably, one copy of either the *UAS-cyt-c-p* or the *UAS-cyt-c-d* transgenes together with one copy of the driver completely rescued the lethality of *cyt-c-p*^{k13905}/*Df*(2L)*Exel6039* flies (Figure 4). We conclude that both cytochrome C proteins of *Drosophila* can function in

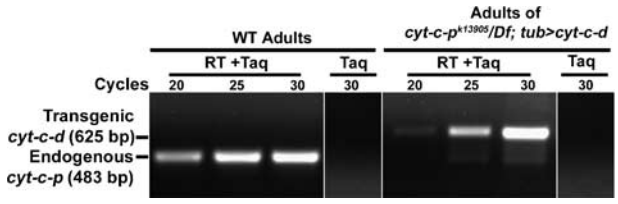

Figure 4 Both *cyt-c-p* and *cyt-c-d* can completely rescue the lethality/respiration defect of *cyt-c-p*$^{-/-}$ embryos. A premix of RT–PCR reaction was designed to amplify endogenous *cyt-c-p* and/or transgenic *cyt-c-d* from testes of wild-type (WT) or rescued *cyt-c-p*$^{-/-}$ adult flies that express transgenic *cyt-c-d* under the control of the *tubulin* promoter (*cyt-c-p*^{k13905}/*Df*(2L)Exel6039*; tub-Gal4/UAS-cyt-c-d*). To confirm that the rescued flies are of the right genotypes, we performed RT–PCR analyses with wild-type and the rescued adult flies using specific primers for the endogenous *cyt-c-p* as well as the transgenic *cyt-c-d*. Note that the strong cytochrome *c* transcript expression in *cyt-c-p*$^{-/-}$ adult flies originated from the *cyt-c-d* transgene.

electron transfer/respiration. The complete absence of *cyt-c-p* from the rescued adult flies is consistent with the idea that *cyt-c-p*^{k13905} is a null allele of *cyt-c-p*. We attribute the faint expression of *cyt-c-p* in *cyt-c-p*^{k13905} homozygote and *cyt-c-p*^{k13905}/*Df*(2L)*Exel6039 trans*-heterozygote mutants detected in early first instar larvae only after 30 PCR cycles (Figure 3F and data not shown) to remnants of maternal contribution. This also explains how *cyt-c-p*$^{-/-}$ mutant embryos can reach the early first instar larval stage without any zygotic contribution. Finally, we could not rescue the lethality of flies homozygous for the *cyt-c-p*^{k13905} allele, suggesting that the *k13905* chromosome carries an additional unrelated lethal mutation.

Immunoreactivity of the cytochrome C-d protein increases at the onset of spermatid individualization

To study the pattern of cytochrome C-d expression in the testis, polyclonal antibodies were raised against four peptides covering the entire length of the protein (see Supplementary data). Consistent with our findings that no *cyt-c-d* RNA is expressed in *cyt-c-d*^{bln1} homozygote flies, almost no signal was detected after staining testes of this mutant with the anti-cytochrome C-d antibody (Figure 5B). Staining wild-type testes with this antibody revealed a grainy pattern of cytochrome C-d signal along the entire length of elongating spermatids and elongated spermatids (Figure 5A). Once an individualization complex (IC) was assembled in the vicinity of the nuclei, an increase in cytochrome C-d staining was detected with the highest intensity found next to the IC (arrowheads in Figure 5C). During the caudal translocation of the IC, a significant portion of cytochrome C-d is depleted from the newly individualized part of the spermatids (arrow in Figure 5C) into the CB (arrowhead in Figure 5D). Eventually, the newly formed WBs accumulate high levels of cytochrome C-d (Figure 5E).

To test whether this antibody could also crossreact with cytochrome C-p, we stained testes *of cyt-c-d* mutant lines that were rescued by transgenic *cyt-c-p* expression in germ cells (described in Figure 2E). Similar to the cytochrome C-d expression in wild type (Figure 5A) or after ectopic expression in mutant testes (Figures 2D and 5H), ectopic cytochrome-C-p expression was also detectable as grainy staining along the entire length of elongated spermatids

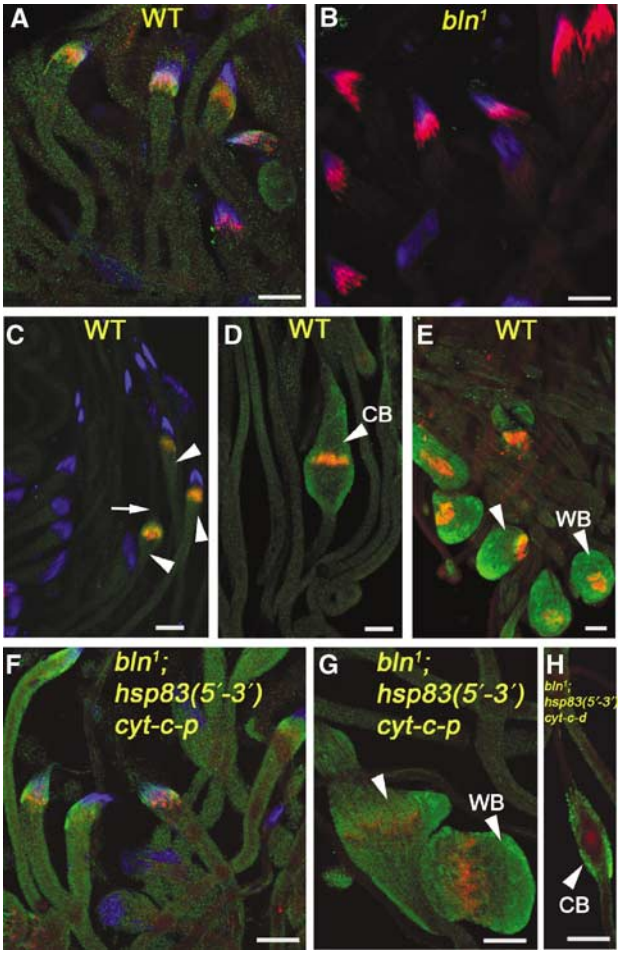

Figure 5 Expression of the testis-specific cytochrome C protein, cytochrome C-d, during spermatogenesis. Nuclei are stained blue (DAPI), and the ICs (which mark the sites of spermatid individualization) are either red or orange (phalloidin). (**A**) In wild-type testis, cytochrome C-d (green) accumulates along the length of elongating and elongated spermatids in a typical mitochondrial grainy pattern, (**B**) while this signal is almost abolished in *cyt-c-d*^{bln1}−/− mutant spermatids. (**C**) The expression of cytochrome C-d becomes more intense after the assembly of the IC with the highest expression detected in the preindividualized region of the spermatids just adjacent to the IC (arrowheads). After the caudal translocation of the IC, the remaining cytochrome C-d is highly reduced in the postindividualized part of the spermatids (white arrow). (**D**) As the IC progresses, the CB (arrowhead) collects the spermatids' bulk cytoplasm and much of the cytochrome C-d from the postindividualized parts of the spermatids. (**E**) Eventually, strong cytochrome C-d signal was detected in the WBs (arrowheads), which contain the discarded cytoplasm. (**F**, **G**) Staining *cyt-c-d* depleted testes (*cyt-c-d*^{bln} −/−), which ectopically express the *cyt-c-p* rescue construct, revealed that the antibodies raised against cytochrome C-d (polyclonal anti-cyt-C-d) can also react with cytochrome C-p. Similar to cytochrome C-d staining in wild type (A), cytochrome C-p expression (green) was detected along the entire length of elongated spermatids (F) and in the WBs (arrowheads in G). (**H**) The ectopically expressed cytochrome C-d is also detected in the rescued *cyt-c-d*^{bln1}−/− mutant testes (arrowhead pointing to a CB). Scale bars 20 μm.

(Figure 5F) as well as in CBs and WBs (arrowheads in Figure 5G). These results demonstrate that the antibody can detect both forms of the *Drosophila* cytochrome C molecules. The lack of staining found in *cyt-c-d*^{bln1} elongating spermatids (Figure 5B) is consistent with the idea that only *cyt-c-d* and not *cyt-c-p* is expressed in mature spermatids.

Mutations in the Drosophila orthologues of the apoptosome components ark and dronc display severe spermatid individualization defects

In vertebrates, mitochondria play an important role in the control of apoptosis by activating the apoptosome, a multiprotein complex that includes caspase-9, Apaf-1, and cytochrome C (Rodriguez and Lazebnik, 1999; Adams and Cory, 2002; Cain *et al*, 2002; Salvesen and Renatus, 2002). *Drosophila* possesses one Apaf-1 orthologue known either as Hac-1 (Zhou *et al*, 1999), Dark (Rodriguez *et al*, 1999), or Dapaf-1 (Kanuka *et al*, 1999) which, like its mammalian counterpart, is important in multiple apoptotic pathways (White, 2000). In addition, *Drosophila* also has a caspase-9 orthologue, Dronc, which, similar to the vertebrate caspase-9, contains a caspase recruitment domain (CARD), and functions in a variety of cell death pathways (Dorstyn *et al*, 1999; Meier *et al*, 2000b; Chew *et al*, 2004; Daish *et al*, 2004; Waldhuber *et al*, 2005; Xu *et al*, 2005). We investigated whether Ark and Dronc are required for spermatid individualization. For this purpose, we examined several EMS-derived loss-of-function alleles of both *ark* and *dronc* (see Materials and methods for more details on the molecular nature of these alleles; M Srivastava and A Bergmann, manuscript in preparation; Xu *et al*, 2005). *ark* and *dronc* mutant flies display highly similar phenotypes and most mutant animals die during pupariation. However, some adult 'escapers' emerge that are both male and female sterile. Both *ark* and *dronc* mutants displayed severe defects during the spermatid individualization process (Figure 6). In particular, *ark* and *dronc* mutant spermatids failed to extrude much of their cytoplasm into a CB, leaving trails of the cytoplasm in what should have been the postindividualized region of the spermatids (white and yellow arrows pointing to 'cytoplasmic trails' in Figure 6B, C, H, and I). Consequently, $ark^{-/-}$ and $dronc^{-/-}$ CBs and WBs are highly reduced in size or appear flat (yellow arrowheads in Figure 6B and H), and frequently a large portion of the spermatids' cytoplasm is retained behind in a 'mini' CB structure (white arrowhead in Figure 6B), which often contains part of the IC (white arrowhead in Figure 6H). The size of the CBs and WBs in *ark* and *dronc* mutants is on average only half the size of their wild-type counterparts (compare Figure 6D and J with Figure 6E, F, K, and L). These phenotypes are reminiscent of testes that ectopically express the caspase inhibitor gene p35 (Arama *et al*, 2003). These results suggest that *ark* and *dronc* are required for normal caspase activation and the initiation of an apoptosis-like process essential for spermatid individualization. However, whereas no caspase-3-like activity was detected in *cyt-c-d*$^{-/-}$ mutants, we could still detect some activation of caspase-3 in *ark* and *dronc* mutant testes (Figure 6B, C, H, and I). This suggests that some of the cytochrome-C-mediated caspase-3 activation is independent of apoptosome components. Alternatively, it is possible that the *ark* and *dronc* alleles used in this study are not complete nulls and therefore retain some residual function that allows a small amount of cytochrome C-induced caspase activation.

Discussion

Cytochrome C is required for caspase activation

In mammals, mitochondria are important for the regulation of apoptosis, and it has been shown that they can release several proapoptotic proteins into the cytosol in response to apoptotic stimuli (Liu *et al*, 1996; Green and Reed, 1998; Larisch *et al*, 2000; Meier *et al*, 2000a; Ravagnan *et al*, 2002; van Loo *et al*, 2002; Kuwana and Newmeyer, 2003). The best-studied case is the release of cytochrome C, an essential component of the respiratory chain. Cytosolic cytochrome C can bind to and activate Apaf-1, which in turn leads to the activation of caspase-9 (Wang, 2001). However, no comparable role of mitochondrial factors for caspase activation has yet been established in invertebrates. We previously reported that the elimination of cytoplasm during terminal differentiation of spermatids in *Drosophila* involves an apoptosis-like process that requires caspase activity, and that a *P*-element insertion (bln^1) in one of the two *Drosophila* cytochrome *c* genes, *cyt-c-d,* is associated with male-sterility and loss of effector caspase activation during spermatid individualization (Arama *et al*, 2003). Similar results were subsequently obtained by another group, but this study suggested that additional genes in the region may contribute to the observed phenotypes (Huh *et al*, 2004). Here, we demonstrate that the defects in caspase activation and spermatid individualization of bln^1 mutant males can be rescued by transgenic expression of the ORF of *cyt-c-d*. Furthermore, from screening more than a thousand male-sterile lines with defects in sperm individualization for defects in active-caspase (CM1) staining, we identified a nonsense point mutation in *cyt-c-d*, which recapitulates all the phenotypes observed for bln^1. Taken together, these results unequivocally demonstrate that *cyt-c-d* is necessary for effector caspase activation and sperm terminal differentiation in *Drosophila*.

cyt-c-p is mostly somatic and cyt-c-d is mainly restricted to the male germ cells

Two decades ago, Limbach and Wu (1985) used the mouse cytochrome *c* gene as a probe for screening a *Drosophila* genomic library and isolated a fragment that carried two distinct cytochrome *c* genes. Northern blot analyses indicated high levels of *cyt-c-p* expression, while *cyt-c-d* was reported to be expressed at much lower levels in all stages of development. However, neither the exon/intron organization nor the boundaries of the 5′ and 3′ UTRs of these genes were determined at the time (for an updated map of the genomic organization, see Arama *et al*, 2003). As a result, the original Northern analyses were performed with a probe corresponding to the untranscribed genomic region between the two cytochrome *c* genes that was not suitable to properly assess the size and distribution of cytochrome *c* transcripts. Unfortunately, this has caused considerable confusion in the field from the start, as even the original report noted that the size of the observed *cyt-c-d* transcript differed more than two-fold from the predicted size (Limbach and Wu, 1985). More recently, relying on the incorrect assumption that *cyt-c-d* is ubiquitously expressed in the fly, Dorstyn *et al* (2004) suggested that a loss-of-function mutation in *cyt-c-d* should lead to severe developmental defects and lethality rather than merely male sterility. However, using a specific *cyt-c-d* 3′ UTR probe reveals a transcript of the predicted size which is absent in *cyt-c-d*^{bln1} mutants (Arama *et al*, 2003). Furthermore, the RT–PCR and immunofluorescence analyses presented here indicate that *cyt-c-d* is mainly expressed in the male germ line and is completely absent during embryonic

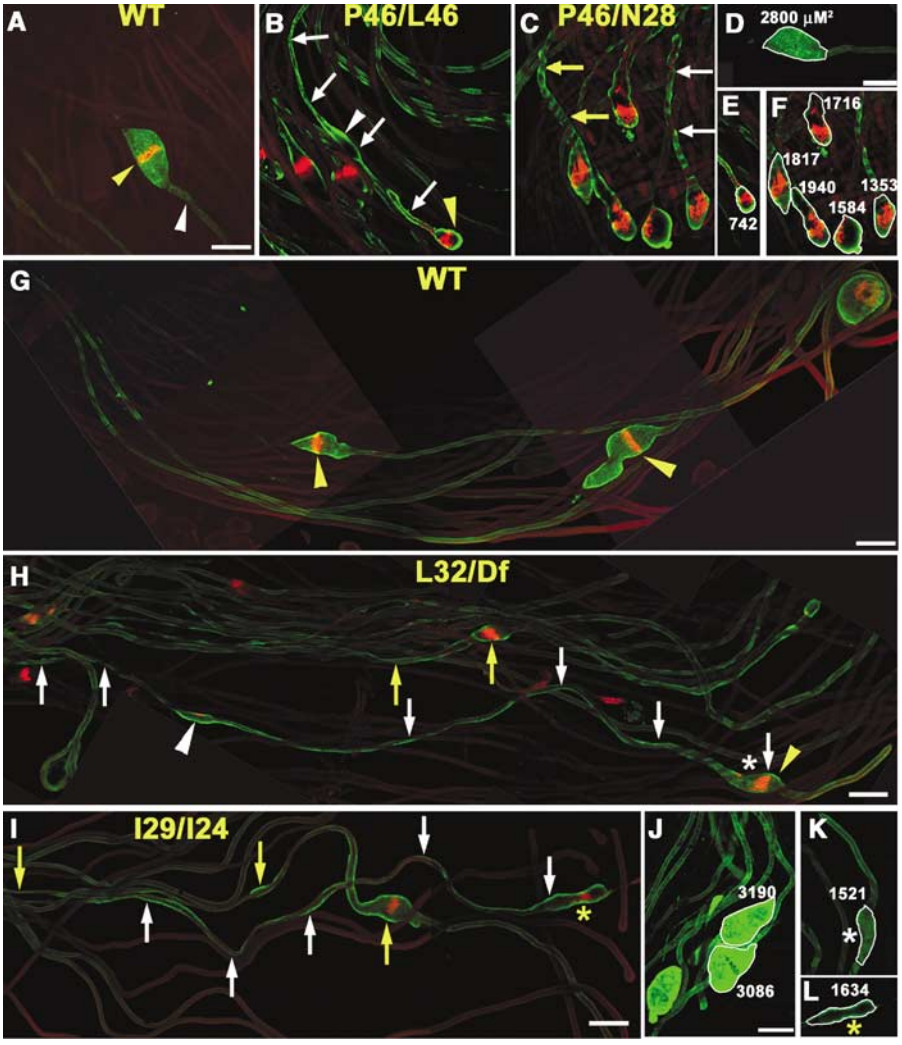

Figure 6 Mutations in *Drosophila* homologues of the apoptosome complex, *ark* and *dronc,* cause spermatid individualization defects. CM1 is in green and the IC appears in red in all the panels. The direction of the caudal individualization movement is from top to bottom (**A, B, C, E, F, J, K**), or from left to right (**D, G, H, I, L**). (G, H, and I) A whole testis view. (A, G) WT CB. The extruded cytoplasm is contained within the oval-shaped CB, which is marked by CM1 staining in green (yellow arrowheads pointing at the ICs within the CBs). Importantly, CM1 staining is absent from the post-individualized portion of the spermatids (above the CB), while it is still apparent in the preindividualized portion (white arrowhead). (B, C) In *ark* and (H, I) *dronc* mutants, the CBs are frequently reduced in size or appear flat (yellow arrowhead in B and H, respectively) due to a failure in the appropriate collection of the cytoplasm of the spermatids. The retained cytoplasm is clearly visualized as a 'trail' of residual cytoplasm (marked by the green CM1 staining) along the entire length of what was supposed to have been the postindividualized portion of the spermatids (B, C and H, I; white or yellow arrows following the 'cytoplasmic trails'). Frequently, a large portion of the spermatids' cytoplasm is retained behind in 'mini' CB structures, which often contain part of the IC (white arrowheads in B, and H). Note that in wild-type testes, 'cytoplasmic trails' do not exist in the post-individualized portion of the spermatids (left to the CBs, which are indicated by yellow arrowheads in G). The surface area of the flattened advanced CBs and WBs in *ark* (E, and F) and *dronc* (K, and L) mutants were measured and compared to the wild-type counterparts (D, and J, respectively). The CBs and WBs in (F) corresponds to the ones in (C), and the WB in (E) corresponds to the WB in (B), which is marked by a yellow arrowhead, asterisks in (K and L) correspond to the asterisks in (H and I), respectively. The actual surface area appears in square micrometer next to the CBs and WBs. Note that the surface area of *ark* and *dronc* mutant WBs vary from cyst to cyst but are always highly reduced compared to wild type. Scale bars 50 μm. (A, B, and C) and (G, H, and I) are displayed in the same magnification.

and larval development, while *cyt-c-p* is expressed in the soma during all stages of development. In light of these findings, it is not surprising that loss-of-function mutations in *cyt-c-d* cause male sterility, whereas *cyt-c-p* mutations lead to embryonic lethality. Our RT–PCR results suggest that *cyt-c-p* is also expressed in the testis, although to a much lower extent than *cyt-c-d*. We attribute this expression primarily to the somatic cells of the testis, since no cytochrome C protein was detected in *cyt-c-d*^{bln1} elongating spermatids, while *cyt-c-p* RNA was shown to be expressed in *cyt-c-d*^{bln1} mutant flies. However, the very low *cyt-c-d* expression detected in the soma of adult females leaves room for the possibility that *cyt-c-d* might function in caspase activation in some somatic cells as well.

A possible conformational change of cytochrome C-d occurs at sites of individualizing spermatids

In mammalian cells, release of cytochrome C into the cytosol in response to proapoptotic stimuli can be readily demonstrated (Von Ahsen *et al*, 2000; Jiang and Wang, 2004).

However, previous attempts to detect a similar phenomenon in *Drosophila* have been unsuccessful (Zimmermann *et al*, 2002; Dorstyn *et al*, 2004). On the other hand, apoptotic stimuli can lead to increased cytochrome C immuno-reactivity (Varkey *et al*, 1999). A possible limitation is that all these studies were conducted using mammalian antibodies with questionable specificity and sensitivity, and only in a small number of cell types and paradigms. Using an antibody that was raised against *Drosophila* cytochrome C-d, we detected an increase in a 'grainy signal' upon the onset of individualization, with the highest staining observed in the vicinity of the IC. Since it is highly unlikely that additional cytochrome C-d is being transcribed and imported to the mitochondria at this late stage, we favor the explanation that a conformational change or an exposure of a hidden epitope causes the increase in the intensity of the signal. The activation of Dronc, the *Drosophila* caspase-9 orthologue, also occurs in association with the IC and depends on the presence of the *Drosophila* Apaf-1 orthologue, Ark (Huh *et al*, 2004). Moreover, the proapoptotic Hid protein is localized in a similar fashion (Huh *et al*, 2004). What are these structures then, which accumulate apoptotic factors in the vicinity of the IC? One plausible suggestion from the literature is that these structures correspond to 'mitochondrial whorls', which result from the extrusion of material from the minor mitochondrial derivative and constitute the leading component of the IC (Tokuyasu *et al*, 1972). These 'whorls' can be labeled using a testes-specific mitochondrial-expressed GFP line (Bazinet and Rollins, 2003; Bazinet, 2004). Using this GFP marker, we found that cytochrome C-d is indeed closely associated with mitochondrial whorls (Supplementary Figure 2). Therefore, it is possible that an active apoptosome forms in the vicinity of the IC in response to dramatic changes in the mitochondrial architecture that occur at this stage of spermatid differentiation. Similarly, studying the response of *Drosophila* flight muscle cells to oxygen stress, Walker and Benzer (2004) have recently reported that the cristae within individual mitochondria become locally rearranged in a pattern that they termed a 'swirl'. This process was associated with widespread apoptotic cell death in the flight muscle, which was correlated with a conformational change of cytochrome C manifested by the display of an otherwise hidden epitope. Collectively, these observations suggest that apoptosome-like complexes composed of cytochrome C-d, Ark, and Dronc might be associated with unique mitochondrial swirl-like structures. Consistent with this idea, we found that the long isoform of Ark that contains theWD40 repeats, the target for cytochrome C binding to mammalian Apaf-1, is the major form detectably expressed in testes (Supplementary Figure 3).

The fact that cytochrome C-d immunoreacitivity increases in the vicinity of the IC suggests that the extensive mitochondrial organizations preceding individualization may be partially required for caspase activation. Consistent with this idea, we isolated several mutants, such as $pln^{Z2-0516}$, which display defects in Nebenkern differentiation and caspase activation (Supplementary Figure 1). However, not all mitochondrial differentiation events are required for caspase activation. For example, CM1 staining is seen in *fuzzy onions*, a mutant defective in the mitochondrial fusion event that generates the Nebenkern (Arama *et al*, 2003). In contrast, analysis of the *pln* mutant indicates that proper elongation of the Nebenkern is essential for caspase activation. Therefore, characterization of other mitochondrial mutants may shed light on the connection between mitochondrial organization and caspase activation during sperm differentiation.

The Drosophila Apaf-1 and caspase-9 orthologues are required for the proper removal of the spermatid cytoplasm during the individualization process

What are the mechanisms by which cytochrome C-d activates caspases during late spermatogenesis? In vertebrate cells, following its release into the cytosol, cytochrome C binds to the WD40 domain of the adaptor molecule Apaf-1, which in turn multimerizes and recruits the initiator caspase, caspase-9 via interaction of their CARD domains. This complex, known as the apoptosome, further cleaves and activates effector caspases like caspase-3 (Shi, 2002). Although this model has become the prevailing dogma in the field, the phenotype of mice mutant for a *Cyt c* with drastically reduced apoptogenic function ('KA allele') suggests that the mechanisms for caspase activation may be more complex than what was previously thought (Hao *et al*, 2005). In particular, this study suggests that cytochrome C-independent mechanisms for the activation of Apaf-1 and caspase-9 exist, as well as cytochrome C-dependent but Apaf-1-independent mechanisms for apoptosis (Green, 2005; Hao *et al*, 2005). Our analyses of *ark* (Apaf-1) and *dronc* (caspase-9) loss-of-function mutants demonstrate that both genes are required for spermatid individualization, and that their phenotypes, in particular their failure to properly remove the spermatid cytoplasm into the WB, resemble *cyt-c-d* mutant spermatids and expression of the caspase inhibitor p35 in the testes. However, we could still detect some caspase-3-like activity in these mutant testes. This may suggest that either the *ark* and *dronc* alleles are not null, or that cytochrome C-d also functions in an apoptosome-independent pathway to promote caspase-3 activation. Therefore, the regulation of caspase activation and apoptosis may be more similar between insects and mammals than has been previously appreciated. Further genetic analysis of this pathway in *Drosophila* may provide general insights into diverse mechanisms of apoptosis activation.

The roles of cytochrome C-d for caspase activation and cytochrome C-p for respiration are interchangeable

Previous observations raised the possibility that the two distinct cytochrome *c* genes may have evolved to serve distinct functions in respiration and caspase regulation (Limbach and Wu, 1985; Inoue *et al*, 1986, Arama *et al*, 2003). In order to address this hypothesis, we asked whether expression of one protein might rescue mutations in the other cytochrome *c* gene. To our surprise, we found that transgenic expression of the *cyt-c-p* ORF in germ cells rescued caspase activation, spermatid individualization, and sterility of *cyt-c-*$d^{-/-}$ flies. Therefore, the ability to activate caspases is not restricted to the cytochrome C-d protein, and it is possible that cytochrome C-p functions in apoptosis in at least some somatic cells.

Although *cyt-c-d* is almost exclusively expressed in the male germ cells, ectopic expression of this protein in the soma can rescue the respiration defect and lethality of *cyt-c-*$p^{-/-}$ mutant flies, demonstrating that cytochrome C-d can

function in energy metabolism. This raises the question whether the lack of caspase activation could be due to reduced ATP-levels. Although this is a formal possibility, we consider this explanation very unlikely since mutant spermatids complete many other energy-intensive cellular processes. These include the extensive transformation from round spermatids to 1.8 mm long elongated spermatids, a process that involves extensive remodeling and movement of actin filaments, generation of the axonemal tail, mitochondrial reorganization, plasma/axonemal membranes reorganization, and nuclear condensation and elongation. Since all of these processes can occur in the absence of cytochrome C-d, there is no overt shortage of ATP in *cyt-c-d* mutants. We therefore consider it very unlikely that ATP has become limiting in these mutant cells. Since earlier stage spermatids express cytochrome C-p (data not shown), sufficient ATP seems to persist to late developmental stages. In mammalian cells, cellular ATP concentration is sufficiently high (around 2 mM) to keep cultured cell alive for several days upon ATP synthase inhibition (Waterhouse *et al*, 2001). Furthermore, cells in which cytochrome *c* expression was decreased by RNAi still underwent apoptosis in response to various stimuli (Zimmermann *et al*, 2002). Likewise, it appears that cytochrome C is not essential for the function of mature murine sperm, since mice deficient for the testis specific form of cytochrome C, Cyt c_T, are fertile (Narisawa *et al*, 2002). Taken together, all these observations argue strongly against the possibility that ATP levels in *cyt-c-d*$^{-/-}$ mutant spermatids would be insufficient for caspase activation.

In conclusion, the results presented here definitively demonstrate that cytochrome C-d is essential for caspase activation and spermatid individualization. Both cytochrome C proteins of *Drosophila* are, at least to some extent, functionally interchangeable. Our results also indicate that cytochrome C can promote caspase activation in the absence of a functional apoptosome. Given the powerful genetic techniques available, late spermatogenesis of *Drosophila* promises to be a powerful system to identify novel pathways for mitochondrial regulation of caspase activation.

Materials and methods

Fly strains

yw flies were used as wild-type controls. The Zuker mutants *Z2-1091*, *Z2-2468*, *Z2-0706,* and *Z2-0516* were obtained from CS Zuker (University of California at San Diego), the *osk*^{301}*/TM3* and *osk*^{CE4}*/TM3* lines from R Lehmann (NYU School of Medicine, NY), *dj*-GFP line 8B from C Bazinet (St. John's University, NY), *bln*^{1} (*blanks*) and *l*(2)*k13905* lines from the Bloomington Stock Center, and the *DF*(2L)Exel6039 line from Exelixis. Both *dronc* and *ark* alleles were isolated from an EMS mutagenesis screen for mutants that recessively suppressed the eye ablation phenotype caused by eye-specific overexpression of hid (Xu *et al*, 2005 and M Srivastava and A Bergmann, paper in preparation). *ark*^{L46} harbors a change of a cysteine to a threonine at position 346 and a premature stop codon at position 950. *ark*^{N28} contains a premature stop codon at position 308. The entire coding region of *ark*^{P46} was sequenced, but no lesions were identified suggesting that it may harbor a mutation in a regulatory element (M Srivastava and A Bergmann, paper in preparation). *dronc*^{I24} and *dronc*^{I29} contain premature stop codons at positions 28 and 53, respectively, and *dronc*^{L32} bears a change of a conserved leucine at position 25 in the CARD domain to glutamic acid (Xu *et al*, 2005).

RNA isolation and RT–PCR

Total RNA was extracted by using the Micro-to-Midi Total RNA Purification System (Invitrogen) according to the manufacturer's recommendations. The amounts of animals or organs used to obtain enough RNA for 5–10 RT–PCR reactions were 20–40 young adult testes or reproductive tracts, 40 larval testes, 10 adult females, 30 young adult ovaries, and 15 first instar larvae. The samples were collected into 1.5 ml Eppendorf tubes, standing on ice and containing 300 µl of the Invitrogen kit's lysis buffer and 3 µl of 2-mercaptoethanol, homogenized using a Pellet Pestle Motor (Kontes), and subsequently purified using the same kit. In the cases when the genomic DNA had to be removed, the 30 µl of the RNA was incubated with 4 µl of RQ1 DNase and 3.8 µl of appropriate buffer (Promega) for 1.5 h at 37°C, and subsequently purified again with the Invitrogen kit. The RNA was stored in −80°C or immediately utilized for RT–PCR reactions using the SuperScript™ III One-Step RT–PCR System with Platinum® *Taq* DNA polymerase (Invitrogen). The Mastercycler Gradient PCR machine (Eppendorf) was programmed as follows: 50°C for 30 min for the RT step followed by 94°C for 2 min, and the amplification steps of 94°C for 30 s, 60°C for 30 s, 68°C for 1 min. A master-mix was prepared and aliquoted to five tubes, each of which was amplified for 17, 20, 25, 30, or 35 cycles. Absence of genomic DNA in RNA preparations was verified by replacing the RT/Taq mix with only *Taq* DNA polymerase (Invitrogen). The comparative RT–PCR reactions in Figure 3 were performed using two pairs of primers in a same reaction mix: For *cyt-c-d* the forward primer GAACAGAATCGGCAGCGGGA and the reverse primer TCTGGATAGCATGGTGGCCG amplified a 543 bp fragment, while for *cyt-c-p* the forward primer GTGAAAAATCGGC GACGCTC and the reverse primer GCGTGCCGGACTGTGACTGA amplified a 483 bp fragment. For amplification of the 625 bp fragment of the transgenic *UAS-cyt-c-d*, the forward primer AGCAAATAAACAAGCGCAGC corresponding to a sequence from the pUASt vector, and the reverse primer CCACGACCCCGCCAA GATTT corresponding to a unique sequence in the ORF of *cyt-c-d* were used. For the RT–PCRs in Figure 1H, we used the following primers: GAACAGAATCGGCAGCGGGA and CCACGACCCCGCCAA GATTT for the 300 bp *cyt-c-d*5′, and CGGTCACTCTGGTCACACTA and GACCGATCAGACCATGCAGA for the 257 bp *cyt-c-p*5′. For the 263 bp *cyt-c-d*3′ the primers used were AAATCTTGGCGGGGTCG TGG and TCTGGATAGCATGGTGGCCG, and for the 323 bp *cyt-c-p*3′ the primers TCTGCATGGTCTGATCGGTC and GTAGTTGTTGCTGCT GCTGC. For the RT–PCRs of the transgenics in Figures 2G and H, we used the forward primer GGGAGCCAACGAGAGAGCGA corresponding to a sequence from the pHSP83(5′–3′UTRs) vector and a reverse primer TCTGGATAGCATGGTGGCCG corresponding to a sequence in the *cyt-c-d* 3′ UTR.

Antibody staining

CM1 antibody staining of young adult testes was carried out essentially as described in Arama *et al* (2003).

Also see online Supplementary_4 for additional Materials and methods.

Supplementary data

Supplementary data are available at *The EMBO Journal* Online.

Acknowledgements

We are deeply indebted to Charles Zuker for sending us their mutant collection, to Barbara Wakimoto for providing us with the annotated list of mutants, and to Maureen Cahill for collecting and shipping the stocks. We are grateful to R Lehmann, E Kurant, C Bazinet, JE Rollins, Exelixis, and the Bloomington stock center for providing additional stocks. We greatly appreciate R Cisse for her technical support in generating the transgenic lines and H Shio for technical assistance with the EM. We thank the Steller lab members for encouragement and advice, and B Mollereau, G Rieckhof, J Rodriguez, S Shaham, and A Tang for critically reading the manuscript. We acknowledge G Rieckhof and A Persaud for assisting with the screen. EA was a fellow of the Charles H Revson Foundation and HS is an investigator with the Howard Hughes Medical Institute. Part of this work was supported by NIH grant RO1 GM60124. AB receives grant support from the NIH (GM068016) and the Robert A Welch Foundation (G1496).

References

Abraham MC, Shaham S (2004) Death without caspases, caspases without death. *Trends Cell Biol* **14:** 184–193

Adams JM, Cory S (2002) Apoptosomes: engines for caspase activation. *Curr Opin Cell Biol* **14:** 715–720

Arama E, Agapite J, Steller H (2003) Caspase activity and a specific cytochrome C are required for sperm differentiation in *Drosophila*. *Dev Cell* **4:** 687–697

Baehrecke EH (2002) How death shapes life during development. *Nat Rev Mol Cell Biol* **3:** 779–787

Baker NE, Yu SY (2001) The EGF receptor defines domains of cell cycle progression and survival to regulate cell number in the developing *Drosophila* eye. *Cell* **104:** 699–708

Bazinet C (2004) Endosymbiotic origins of sex. *Bioessays* **26:** 558–566

Bazinet C, Rollins JE (2003) Rickettsia-like mitochondrial motility in *Drosophila* spermiogenesis. *Evol Dev* **5:** 379–385

Benedict MA, Hu Y, Inohara N, Nunez G (2000) Expression and functional analysis of Apaf-1 isoforms. Extra Wd-40 repeat is required for cytochrome *c* binding and regulated activation of procaspase-9. *J Biol Chem* **275:** 8461–8468

Brand AH, Perrimon N (1993) Targeted gene expression as a means of altering cell fates and generating dominant phenotypes. *Development* **118:** 401–415

Cain K, Bratton SB, Cohen GM (2002) The Apaf-1 apoptosome: a large caspase-activating complex. *Biochimie* **84:** 203–214

Chew SK, Akdemir F, Chen P, Lu WJ, Mills K, Daish T, Kumar S, Rodriguez A, Abrams JM (2004) The apical caspase dronc governs programmed and unprogrammed cell death in *Drosophila*. *Dev Cell* **7:** 897–907

Daish TJ, Mills K, Kumar S (2004) *Drosophila* caspase DRONC is required for specific developmental cell death pathways and stress-induced apoptosis. *Dev Cell* **7:** 909–915

Degterev A, Boyce M, Yuan J (2003) A decade of caspases. *Oncogene* **22:** 8543–8567

Dorstyn L, Colussi PA, Quinn LM, Richardson H, Kumar S (1999) DRONC, an ecdysone-inducible *Drosophila* caspase. *Proc Natl Acad Sci USA* **96:** 4307–4312

Dorstyn L, Mills K, Lazebnik Y, Kumar S (2004) The two cytochrome c species, DC3 and DC4, are not required for caspase activation and apoptosis in *Drosophila* cells. *J Cell Biol* **167:** 405–410

Dorstyn L, Read S, Cakouros D, Huh JR, Hay BA, Kumar S (2002) The role of cytochrome *c* in caspase activation in *Drosophila melanogaster* cells. *J Cell Biol* **156:** 1089–1098

Fraser AG, McCarthy NJ, Evan GI (1997) drICE is an essential caspase required for apoptotic activity in *Drosophila* cells. *EMBO J* **16:** 6192–6199

Green DR (2005) Apoptotic pathways: ten minutes to dead. *Cell* **121:** 671–674

Green DR, Reed JC (1998) Mitochondria and apoptosis. *Science* **281:** 1309–1312

Hao Z, Duncan GS, Chang CC, Elia A, Fang M, Wakeham A, Okada H, Calzascia T, Jang Y, You-Ten A, Yeh WC, Ohashi P, Wang X, Mak TW (2005) Specific ablation of the apoptotic functions of cytochrome *c* reveals a differential requirement for cytochrome *c* and Apaf-1 in apoptosis. *Cell* **121:** 579–591

Hengartner MO (2000) The biochemistry of apoptosis. *Nature* **407:** 770–776

Huh JR, Vernooy SY, Yu H, Yan N, Shi Y, Guo M, Hay BA (2004) Multiple apoptotic caspase cascades are required in nonapoptotic roles for *Drosophila* spermatid individualization. *PLoS Biol* **2:** E15

Inoue S, Inoue H, Hiroyoshi T, Matsubara H, Yamanaka T (1986) Developmental variation and amino acid sequences of cytochromes c of the fruit fly *Drosophila melanogaster* and the flesh fly *Boettcherisca peregrina*. *J Biochem (Tokyo)* **100:** 955–965

Jacobson MD, Weil M, Raff MC (1997) Programmed cell death in animal development. *Cell* **88:** 347–354

Jiang X, Wang X (2004) Cytochrome C-mediated apoptosis. *Annu Rev Biochem* **73:** 87–106

Kanuka H, Sawamoto K, Inohara N, Matsuno K, Okano H, Miura M (1999) Control of the cell death pathway by Dapaf-1, a *Drosophila* Apaf-1/CED-4-related caspase activator. *Mol Cell* **4:** 757–769

Kornbluth S, White K (2005) Apoptosis in *Drosophila*: neither fish nor fowl (nor man, nor worm). *J Cell Sci* **118:** 1779–1787

Koundakjian EJ, Cowan DM, Hardy RW, Becker AH (2004) The Zuker collection: a resource for the analysis of autosomal gene function in *Drosophila melanogaster*. *Genetics* **167:** 203–206

Kuwana T, Newmeyer DD (2003) Bcl-2-family proteins and the role of mitochondria in apoptosis. *Curr Opin Cell Biol* **15:** 691–699

Larisch S, Yi Y, Lotan R, Kerner H, Eimerl S, Tony PW, Gottfried Y, Birkey RS, de Caestecker MP, Danielpour D, Book-Melamed N, Timberg R, Duckett CS, Lechleider RJ, Steller H, Orly J, Kim SJ, Roberts AB (2000) A novel mitochondrial septin-like protein, ARTS, mediates apoptosis dependent on its P-loop motif. *Nat Cell Biol* **2:** 915–921

Limbach KJ, Wu R (1985) Characterization of two *Drosophila melanogaster* cytochrome c genes and their transcripts. *Nucleic Acids Res* **13:** 631–644

Liu X, Kim CN, Yang J, Jemmerson R, Wang X (1996) Induction of apoptotic program in cell-free extracts: requirement for dATP and cytochrome *c*. *Cell* **86:** 147–157

Meier P, Finch A, Evan G (2000a) Apoptosis in development. *Nature* **407:** 796–801

Meier P, Silke J, Leevers SJ, Evan GI (2000b) The *Drosophila* caspase DRONC is regulated by DIAP1. *EMBO J* **19:** 598–611

Narisawa S, Hecht NB, Goldberg E, Boatright KM, Reed JC, Millan JL (2002) Testis-specific cytochrome *c*-null mice produce functional sperm but undergo early testicular atrophy. *Mol Cell Biol* **22:** 5554–5562

Nelson DA, White E (2004) Exploiting different ways to die. *Genes Dev* **18:** 1223–1226

Peterson JS, Barkett M, McCall K (2003) Stage-specific regulation of caspase activity in *Drosophila* oogenesis. *Dev Biol* **260:** 113–123

Ravagnan L, Roumier T, Kroemer G (2002) Mitochondria, the killer organelles and their weapons. *J Cell Physiol* **192:** 131–137

Riedl SJ, Shi Y (2004) Molecular mechanisms of caspase regulation during apoptosis. *Nat Rev Mol Cell Biol* **5:** 897–907

Rodriguez A, Oliver H, Zou H, Chen P, Wang X, Abrams JM (1999) Dark is a *Drosophila* homologue of Apaf-1/CED-4 and functions in an evolutionarily conserved death pathway. *Nat Cell Biol* **1:** 272–279

Rodriguez J, Lazebnik Y (1999) Caspase-9 and APAF-1 form an active holoenzyme. *Genes Dev* **13:** 3179–3184

Salvesen GS (2002) Caspases and apoptosis. *Essays Biochem* **38:** 9–19

Salvesen GS, Abrams JM (2004) Caspase activation—stepping on the gas or releasing the brakes? Lessons from humans and flies. *Oncogene* **23:** 2774–2784

Salvesen GS, Renatus M (2002) Apoptosome: the seven-spoked death machine. *Dev Cell* **2:** 256–257

Shi Y (2002) Mechanisms of caspase activation and inhibition during apoptosis. *Mol Cell* **9:** 459–470

Slee EA, Harte MT, Kluck RM, Wolf BB, Casiano CA, Newmeyer DD, Wang HG, Reed JC, Nicholson DW, Alnemri ES, Green DR, Martin SJ (1999) Ordering the cytochrome c-initiated caspase cascade: hierarchical activation of caspases-2, -3, -6, -7, -8, and -10 in a caspase-9-dependent manner. *J Cell Biol* **144:** 281–292

Song Z, Steller H (1999) Death by design: mechanism and control of apoptosis. *Trends Cell Biol* **9:** M49–M52

Thompson CB (1995) Apoptosis in the pathogenesis and treatment of disease. *Science* **267:** 1456–1462

Tokuyasu KT, Peacock WJ, Hardy RW (1972) Dynamics of spermiogenesis in *Drosophila melanogaster*. I. Individualization process. *Z Zellforsch Mikrosk Anat* **124:** 479–506

van Loo G, Saelens X, van Gurp M, MacFarlane M, Martin SJ, Vandenabeele P (2002) The role of mitochondrial factors in apoptosis: a Russian roulette with more than one bullet. *Cell Death Differ* **9:** 1031–1042

Varkey J, Chen P, Jemmerson R, Abrams JM (1999) Altered cytochrome c display precedes apoptotic cell death in *Drosophila*. *J Cell Biol* **144:** 701–710

Von Ahsen O, Waterhouse NJ, Kuwana T, Newmeyer DD, Green DR (2000) The 'harmless' release of cytochrome *c*. *Cell Death Differ* **7:** 1192–1199

Wakimoto BT, Lindsley DL, Herrera C (2004) Toward a comprehensive genetic analysis of male fertility in *Drosophila melanogaster*. *Genetics* **167:** 207–216

Waldhuber M, Emoto K, Petritsch C (2005) The *Drosophila* caspase DRONC is required for metamorphosis and cell death in response to irradiation and developmental signals. *Mech Dev* **122:** 914–927

Walker DW, Benzer S (2004) Mitochondrial 'swirls' induced by oxygen stress and in the *Drosophila* mutant hyperswirl. *Proc Natl Acad Sci USA* **101:** 10290–10295

Wang X (2001) The expanding role of mitochondria in apoptosis. *Genes Dev* **15:** 2922–2933

Waterhouse NJ, Goldstein JC, von AO, Schuler M, Newmeyer DD, Green DR (2001) Cytochrome *c* maintains mitochondrial transmembrane potential and ATP generation after outer mitochondrial membrane permeabilization during the apoptotic process. *J Cell Biol* **153:** 319–328

White K (2000) Cell death: *Drosophila* Apaf-1—no longer in the (d)Ark. *Curr Biol* **10:** R167–R169

Xu D, Li Y, Arcaro M, Lackey M, Bergmann A (2005) The CARD-carrying caspase Dronc is essential for most, but not all, developmental cell death in *Drosophila*. *Development* **132:** 2125–2134

Zhou L, Song Z, Tittel J, Steller H (1999) HAC-1, a *Drosophila* homolog of APAF-1 and CED-4 functions in developmental and radiation-induced apoptosis. *Mol Cell* **4:** 745–755

Zimmermann KC, Ricci JE, Droin NM, Green DR (2002) The role of ARK in stress-induced apoptosis in *Drosophila* cells. *J Cell Biol* **156:** 1077–1087

Zou H, Henzel WJ, Liu X, Lutschg A, Wang X (1997) Apaf-1, a human protein homologous to *C. elegans* CED-4, participates in cytochrome *c*-dependent activation of caspase-3. *Cell* **90:** 405–413

Supplementary_1

Results

Mutations that affect the Nebenkern, a unique mitochondrial formation, block caspase activation and spermatid individualization

The requirement of cytochrome C-d for caspase activation during spermatid individualization provides a link between this apoptosis-like process and mitochondrial function. Because sperm in insects, such as *Drosophila*, carry a unique mitochondrial formation, known as the Nebenkern, we were interested in further exploring this connection. Immediately after completion of meiosis, the mitochondria of the spermatid assemble on one side of the haploid pronucleus and fuse together into two giant aggregates (Fuller, 1993). These aggregated mitochondria then wrap around one another to produce the spherical Nebenkern (yellow arrows in Supplementary Figure 1C). When viewed in cross-section under the transmission electron microscope, the Nebenkern resembles a sliced onion, and hence this early stage of spermatogenesis is called the "onion stage". When the flagellum elongates, the two mitochondrial regions of the Nebenkern unfold and elongate down the side of the 1.8 mm long axoneme (Supplementary Figure 1E-G and K-N; Fuller, 1993). However, while the use of electron microscopy facilitated a detailed and insightful morphological description of this extensive mitochondrial organization (Tokuyasu, 1974; Tokuyasu, 1975), the role of the Nebenkern for the development of the spermatid is still unknown. Interestingly, in addition to a block in caspase activation, almost a third of the mutants identified in the genetic screen (described in the "Results" section) also displayed severe defects in Nebenkern organization (Supplementary Figure 1 and data not shown). In contrast, we previously reported that the *fuzzy onions* mutant, which blocks mitochondrial fusion but not elongation (Hales and Fuller, 1997) still displayed caspase activation (Arama *et al*, 2003). Thus, to shed light on the specific Nebenkern organization property required for caspase activation, we extensively analyzed the morphological defect of the mitochondria of one of these mutants, which we called *pln* (because the defective mitochondrial derivatives in these spermatids are aggregated in a "neck"-like region immediately adjacent to the nucleus as seen in Supplementary Figure 1J, which is reminiscent of the

Pa Dong **L**ong **N**eck women who live along the Thai and Burmese border; this mutant corresponds to Zuker stock #*Z2-0516*). Using phase-contrast microscopy, we found that while no gross mitochondrial defects were observed during early stages of spermatocyte development (data not shown), a pronounced defect of grainy and highly vacuolated Nebenkerns was observed in $pln^{Z2\text{-}0516}$ round spermatids (compare Supplementary Figure 1C and D). Staining testes with DAPI, which binds to both nuclear and mitochondrial DNA also reveals the smooth versus grainy Nebenkerns in wild-type and $pln^{Z2\text{-}0516}$ round spermatids, respectively (yellow arrows in Supplementary Figure 1E and H). Furthermore, in $pln^{Z2\text{-}0516}$ mutants, the Nebenkerns fail to elongate, displaying non-homogeneous agglomerations of mitochondrial DNA adjacent to the nuclear pole (compare Supplementary Figure 1F and G with I and J). To obtain a more accurate characterization of the mitochondrial defect in *pln* mutants and to confirm the mitochondrial elongation defect observed, we used transmission electron microscopy. In wild-type, the elongating Nebenkern splits into the major and the minor mitochondrial derivatives (red and blue, respectively in Supplementary Figure 1K-N), which are associated with the axoneme (green) throughout the entire period of flagellar elongation. As the spermatids mature, the volume of the minor derivative is reduced until after individualization when it becomes a tiny wedge (blue in Supplementary Figure 1N). Meanwhile, as the major derivative matures, it accumulates an amorphic material known as the "paracrystalline" material (dark mitochondrial density in Supplementary Figure 1L-N). In $pln^{Z2\text{-}0516}$ spermatids however, most of the axonemes (green in Supplementary Figure 1O-R) are not associated at all or only sometimes associated with only one mitochondrial derivative with no "paracrystalline" material inside (yellow in Supplementary Figure 1O-Q). In addition, we frequently observed immature mitochondrial derivatives, which fail to unfurl properly resembling the early onion-like shaped Nebenkern in round spermatids (purple in Supplementary Figure 1P and R). These results demonstrate that *pln* is required for Nebenkern elongation and that disruption of this process causes a block in caspase activation. Hence, we have established a link between mitochondrial reorganization and caspase activation in *Drosophila* spermatids.

Sup. Figure 1

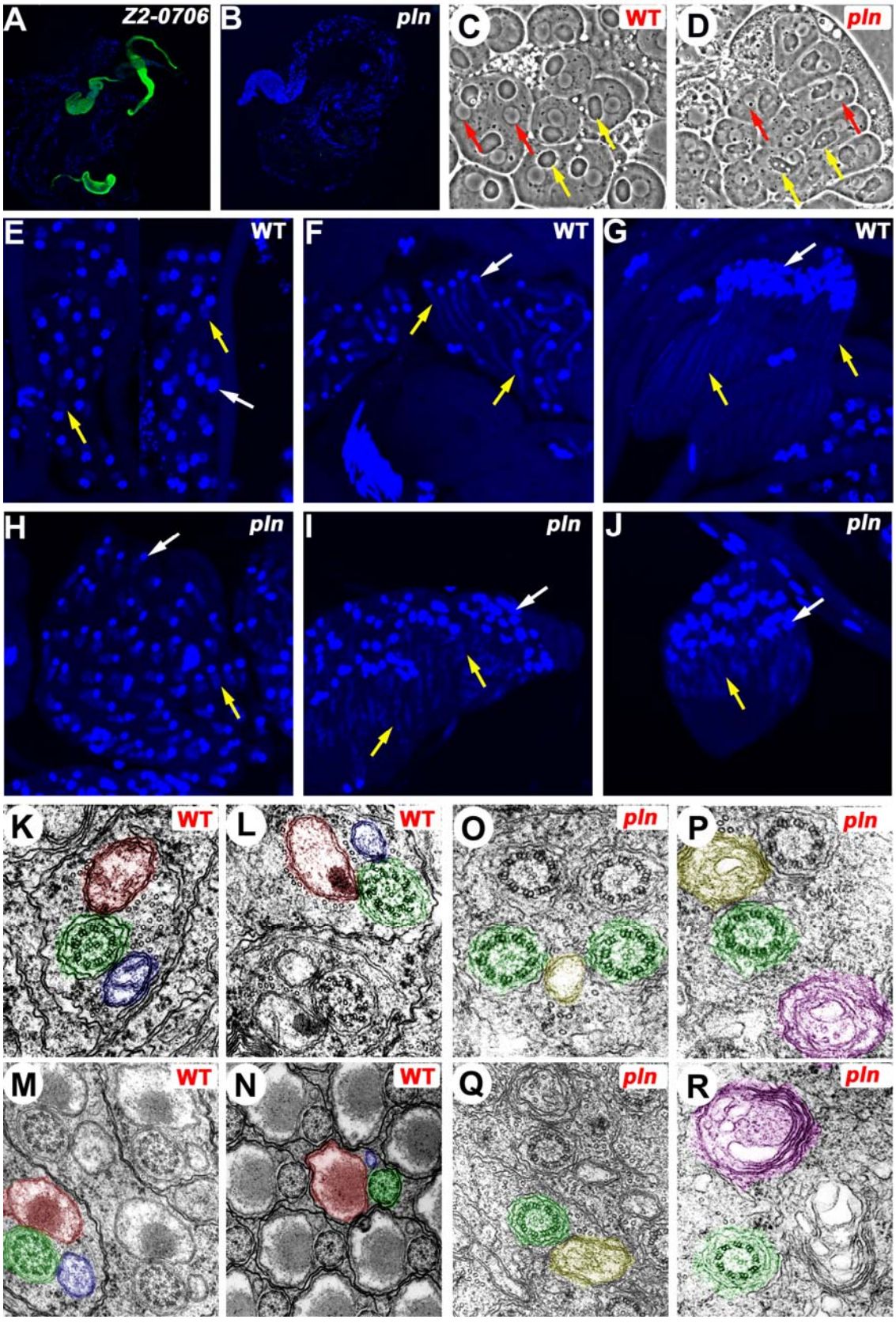
A
Z2-0706
B
pln
C
WT
D
pln
E
WT
F
WT
G
WT
H
pln
I
pln
J
pln
K
WT
L
WT
O
pln
P
pln
M
WT
N
WT
Q
pln
R
pln

Sup_1 Mutations which affect mitochondrial organization block caspase activation and spermatid individualization. (**A**) While CM1 staining is clearly visualized (green) in testes of a representative mutant (*Z2-0706*) that displays a strong block in mid spermatid elongation stage, (**B**) no CM1 staining was detected in the *pln* mutants. The nuclei (blue) are stained with DAPI. (**C**) Round spermatids from wild-type flies visualized by phase microscopy. The mitochondria fuse into a giant mitochondrion, known as the Nebenkern (yellow arrows) which is about the same diameter as the nucleus (red arrows). Note the smooth oval shape of the Nebenkern. (**D**) In contrast, the Nebenkern in round spermatids of *pln* mutants are grainy and highly vacuolated (yellow arrows). Using DAPI to stain nuclei and mitochondrial DNA also indicates that in wild-type the mitochondrial DNA in Nebenkerns (**E**, weak blue, yellow arrows) and in the elongating mitochondrial derivatives (**F, G,** yellow arrows) appear smooth and homogenous, while in $pln^{Z2\text{-}0516}$ -/- round spermatids' Nebenkerns the DNA is grainy (**H**, yellow arrows) and later fails to elongate properly, displaying non-homogeneous agglomerations of mitochondrial DNA (**I, J,** yellow arrows). (**K-R**) Electron micrographs of cross sections through elongating spermatids. The colors indicated were manually added using Adobe Photoshop program to emphasize the described organelles. (**K-N**) In wild-type, as the Nebenkern elongates, it splits into two parts; the major (red) and the minor (blue) mitochondrial derivatives. Note that the minor derivative is reduced as the spermatids mature until it becomes a tiny wedge after individualization (blue in N). The two mitochondrial derivatives assume a characteristic angular relationship with the axoneme (green) throughout the period of flagellar elongation. (**O-R**) In $pln^{Z2\text{-}0516}$ -/- elongating spermatids, no or only one out of the two mitochondrial derivatives (yellow) is visualized in association with the axoneme (green). Furthermore, immature mitochondrial derivatives, which fail to unfurl properly, is frequently visualized (purple). The magnification of the electron micrographs is 50,000.

References

Fuller MT (1993). Spermatogenesis in *Drosophila*. In Bate,M. and Arias,A.M. (Eds.), *The Development of Drosophila melanogaster*, . Cold Spring Harbor Laboratory Press, pp. 71-147.

Hales KG, Fuller MT (1997) Developmentally regulated mitochondrial fusion mediated by a conserved, novel, predicted GTPase. *Cell* **90:** 121-129

Tokuyasu KT (1974) Dynamics of spermiogenesis in Drosophila melanogaster. 3. Relation between axoneme and mitochondrial derivatives. *Exp Cell Res* **84:** 239-250

Tokuyasu KT (1975) Dynamics of spermiogenesis in Drosophila melanogaster. VI. Significance of "onion" nebenkern formation. *J Ultrastruct Res* **53:** 93-112

Supplementary_2

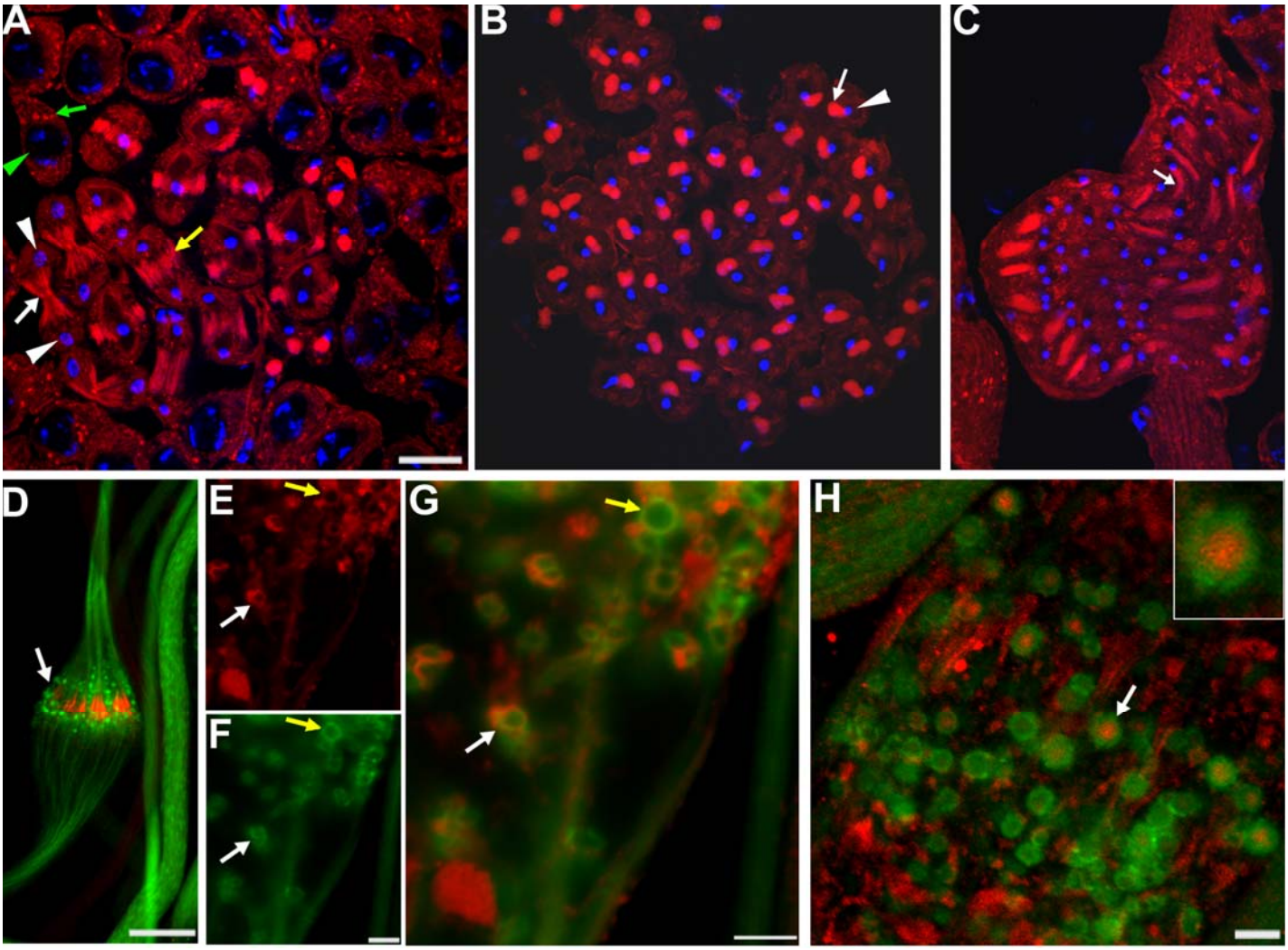

Sup_2 Cytochrome C-d is closely associated with mitochondrial whorls within cystic bulges. (**A-C**) MitoFluor Red 589 dye (red) allows the visualization of the mitochondria during spermatogenesis. The nuclei (blue) are stained with DAPI. (**A**) In primary spermatocytes (green arrowhead pointing to the typical spermatocyte nucleus, consisting of three masses of chromatin), the mitochondria are scattered in the cytoplasm (green arrow). During meiosis, the mitochondria aggregate along the cell equator (yellow arrow), and then during cytokinesis, they divide and segregate equally between the two daughter cells (white arrow points at dividing mitochondria; white arrowheads are pointing at the nuclei of the two daughter cells). (**B**) In round spermatids, the mitochondria fuse into a giant mitochondrion known as the Nebenkern (arrow; arrowhead is pointing at the adjacent nucleus). (**C**) In early elongating spermatids, the elongating mitochondrial derivative (arrow) acquires a comet-like shape.

(**D**) Don Juan (DJ) protein is associated with mitochondria of elongated spermatids at the onset of individualization (Santel *et al*, 1998). During spermatid individualization (arrow pointing at an advanced cystic bulge), DJ-GFP fusion protein accumulates in round structures (green dots; *dj*-expressing bodies) located in the vicinity of the individualization complex (IC; phalloidin; red). It is presumed that these *dj*-expressing bodies correspond to “mitochondrial whorls”, which result from the extrusion of material from the minor mitochondrial derivative (Bazinet and Rollins, 2003; for more details on the minor mitochondrial derivative dynamics see Supplementary_1). (**E-G**) Higher magnification of the IC region of an advanced cystic bulge reveals that the MitoFluor Red 589 dye (**E, G**; red) also accumulates in these 3 µm diameter, doughnut-shaped, *dj*-expressing bodies (**F, G**; green), therefore, further confirming their mitochondrial origin (white and yellow arrows in **E-G** are pointing at the same structures, respectively). (**H**) Finally, cytochrome C-d (red) is associated with the inner compartment of the *dj*-expressing body (green). The *dj*-expressing body in the inset corresponds to the one marked by an arrow. Analyses of serial optical sections within this region suggest that cytochrome C-d accumulates only in one side of the *dj*-expressing bodies.

Scale bars in **A** and **D** 20 µm. **A, B,** and **C** are displayed in the same magnification. Scale bars in **F-H** 5 µm.

References

Bazinet C, Rollins JE (2003) Rickettsia-like mitochondrial motility in Drosophila spermiogenesis. *Evol Dev* **5:** 379-385

Santel A, Blumer N, Kampfer M, Renkawitz-Pohl R (1998) Flagellar mitochondrial association of the male-specific Don Juan protein in Drosophila spermatozoa. *J Cell Sci* **111:** 3299-3309

Supplementary_3

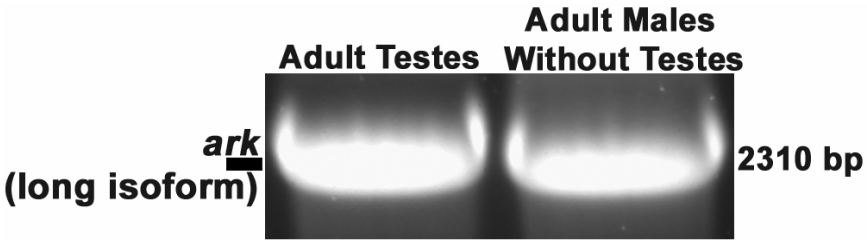

Sup_3 Expression of the long isoform of *ark* in the testes and the soma. After reverse transcription with RNA from adult testes and adult males that had their testes removed, PCR was performed using specific primers for the long isoform of *ark*. The long Ark isoform contains the WD40 repeat domain, which is the target for cytochrome C binding to mammalian Apaf-1.

We used the following primers that flank either a 2310 bp long *ark* cDNA or 2655 bp long *ark* genomic DNA:

Forward:5’-ATCATTGAGAGCTCTCTAAACGTTCTGGAG-3’

Reverse:5’-GTGGTCGGAAAACAAAATGATATACTGTCC-3’

Supplementary_4

Materials and methods

Fly strains and expression vectors

Standard *Drosophila* techniques were used to generate transgenic lines from the following constructs: For the *hsp83(5'-3'UTRs)* lines, a 338 bp fragment from the 5' UTR and a 197 bp fragment from the 3' UTR of *cyt-c-d* were PCR amplified from the BDGP's EST clone LP05614 and subcloned in a subsequent order into the *Xho*I + *Eco*RI and *Bam*HI + *Not*I sites, respectively, of the CasperR-HSP83 vector (Horabin and Schedl, 1993) to obtain the pHSP83(5'-3'UTRs) vector. For the *hsp83(5'-3'UTRs)-cyt-c-d* and *hsp83(5'-3'UTRs)-cyt-c-p* lines, we PCR amplified the *cyt-c-d* and *cyt-c-p* ORFs from the BDGP's EST clones LP05614 and RH17228, respectively, digested the PCR products with *Eco*RI + *Bgl*II, and ligated them into the E*co*RI + B*am*HI sites of the pHSP83(5'-3'UTRs) vector. For the *UAS-cyt-c-d* and *UAS-cyt-c-p* lines, the clones LP05614 and RH17228, respectively, were digested with *Eco*RI and *Xho*I (for *cyt-c-d*) or *Acc*65I (for *cyt-c-p*), and the fragments containing the *cyt-c-d* and *cyt-c-p* coding regions were ligated into the *Eco*RI and *Xho*I or *Acc*65I sites, respectively, of the pUASt vector (Brand *et al*, 1993).

Genetic screen of the "Zuker" male sterile collection lines

A list of more than one thousand male sterile lines with defects during late spermatogenesis was obtained from Barbara Wakimoto (University of Washington). These flies were obtained from Charles Zuker (University of California at San Diego), and for each line the testes of at least three homozygous males were dissected in testis buffer (10mM Tris-Hcl [pH 6.8], 183 mM KCl, 47 mM NaCl, 1 mM EDTA, and 1 mM PMSF) and placed in fixative made of 4% formaldehyde in PBX (PBS + 0.1% Triton X-100) in a MultiScreen 96 well filter plates (MADVN6510, Millipore), standing on ice. After dissections, the plate was rocked for 20 min at RT. Solutions in all the wells are being changed simultaneously using vacuum filtration (Millipore). Testes were washed three times in PBX for 10 min, blocked with PBS/BSA (1% BSA in PBS) for 45 min, incubated with 100 μl of the CM1 antibody (diluted 1:75 in PBS/BSA) overnight at 4^{o}C,

and washed three times with PBX for 10 min. Testes were incubated with 100 μl of the secondary antibody (biotinylated universal antibody diluted 1:50 in PBS/BSA, Vectastain, Vector) for 1 hr, washed three times in PBX for 10 min, and the colorimetric assay was developed using the Vectastain kit (Vector) according to manufacture's recommendations and DAB (Fast DAB tablet set, Sigma). The reaction was stopped by washing twice with 120 mM Tris-HCl.

Antibody staining

CM1 antibody staining of young (0-2 day old) adult testes was carried out (as described in Arama *et al*, 2003) using a rabbit polyclonal anti-Cleaved Caspase-3 (Asp175) antibody (CM1, Cell Signaling Technology, Cat. # 9661) diluted 1:75. The only exceptions are that the subsequent TRITC-phalloidin (Sigma) incubation for staining the ICs was carried out for 5 min in room temperature, and the slides were subsequently rinsed twice for 10 min in PBS.

To generate the anti-Cyt-c-d antibody, four peptides corresponding to the entire cytochrome C-d protein length have been synthesized, purified, conjugated to KLH, and injected together to the same rabbits. Part of the 2nd bleed has been purified on an affinity column coupled to a mixture of all the four peptides (Alpha Diagnostic International). The anti-Cyt-c-d antibody (diluted 1:10 for the affinity purified or 1:400 for the non purified) was used to stain young adult testes (essentially as described in Hime *et al*, 1996). Secondary anti-rabbit antibodies were purchased from Jackson ImmunoResearch Laboratories.

Mitochondrial staining

Wild-type or *dj*-GFP transgenic fly testes were dissected and fixed in formaldehyde (as described in Arama *et al*, 2003). Following fixation the slides were rinsed in PBS, and the tissues were incubated for 20 min in PBS containing 200 nM of the MitoFluor Red 589 probe (Molecular Probes). Then, the slides were washed once with PBS, and mounted in Vectashield mounting medium with DAPI (Vector Laboratories).

Isolation of genomic DNA and PCR

Genomic DNA was isolated from 25-50 adult flies using the High Pure PCR Template Preparation Kit (Roche). Two μg of genomic DNA were used to amplify the *cyt-c-d* or *cyt-c-p* coding regions from wild-type and *cyt-c-d*$^{Z2\text{-}1091}$ homozygotes in a PCR reaction. The pairs of primers used are indicated above for the comparative RT-PCRs. PCR reactions were carried out using DyNAzyme EXT DNA polymerase (Finnzymes), according to the manufacturer instructions. The products were purified using the High Pure PCR Product Purification Kit (Roche), concentrated by evaporation, and sequenced in the Rockefeller University sequencing facility. A similar procedure was carried out to confirm the presence of the transgenes (Figure 2F).

DEVDase activity assay

124 testes were dissected from newly eclosed wild-type or *cyt-c-d*$^{Z2\text{-}1091}$ homozygote males, collected into 1.5 ml Eppendorf tubes, standing on ice and containing 150 μl of testis buffer (10 mM Tris-HCl [pH 6.8], 183 mM KCl, 47 mM NaCl, 1mM EDTA, and 1 mM PMSF), homogenized using a Pellet Pestle Motor (Kontes), and subsequently equally divided into two tubes. Either Z-VAD (20 μM final concentration; Enzyme Systems Products) or DMSO was added to each tube, and the samples were transferred to a 96 well assay white plate (Costar #3610, Corning Inc), and allowed to incubate for 10 min at RT. Caspase-Glo 3/7 reagent (Promega) was added to a final volume of 200 μl and the signal was detected with a multiwell plate reader (SPECTRA max M2, Molecular Devices). Luminescence readings were obtained every two minutes; therefore, each time interval in the figure represents an average of five readings. Three similar experiments were performed that gave similar results.

Examination of testis contents by phase-contrast microscopy

Testes from newly eclosed wild-type or *pln*$^{Z2\text{-}0516}$ homozygote males were placed on a glass slide with a drop of PBS. The testes were torn open and gently squashed under the weight of a cover slip and were taken immediately to visualize under the microscope.

Ultrastructural studies

Wild-type and *pln* mutant testes were dissected in chilled glutaraldehyde (2.5% in 0.1 M cacodylic buffer, pH 7.4) and fixed on ice. The testes were post-fixed in 1% osmium tetroxide in the same buffer on ice, dehydrated in graded concentrations of ethanol, stained *en* bloc with uranyl acetate, and embedded in Epon. For the transmission electron microscopy (TEM), ultra-thin sections were cut on a Reichert-Jung Ultracut E microtome and poststained with uranyl acetate and lead citrate. Sections were examined and photographed on a JEOL100CXII at 80 kV.

References

Arama E, Agapite J, Steller H (2003) Caspase activity and a specific cytochrome C are required for sperm differentiation in Drosophila. *Dev Cell* **4:** 687-697

Brand AH, Perrimon N (1993) Targeted gene expression as a means of altering cell fates and generating dominant phenotypes. *Development* **118:** 401-415

Hime GR, Brill JA, Fuller MT (1996) Assembly of ring canals in the male germ line from structural components of the contractile ring. *J Cell Sci* **109 (Pt 12):** 2779-2788

Horabin JI, Schedl P (1993) Sex-lethal autoregulation requires multiple cis-acting elements upstream and downstream of the male exon and appears to depend largely on controlling the use of the male exon 5' splice site. *Mol Cell Biol* **13:** 7734-7746